Dynamic Shear Behavior of a Needle-Punched Geosynthetic Clay Liner/ Geomembrane Interface at a High Normal Stress

A Thesis

Presented in Partial Fulfillment of the Requirements for

Graduation with Distinction with the Degree of Bachelor of Science

in the Civil Engineering Department of the

College of Engineering of The Ohio State University

By

Alexander Nicholas Stern

The Ohio State University

2009

Undergraduate Honors Examination Committee: Approved by:

Dr. Patrick Fox, Advisor _____

Dr. Halil Sezen Advisor

Civil Engineering Undergraduate Honors Program

ABSTRACT

Geosynthetics are used in waste containment applications in landfills across the world, including seismic regions. The investigation of the interface shear strength of a geomembrane (GM) and a geosynthetic clay liner (GCL) under cyclic motion is needed in order to better understand its response to dynamic loading (e.g. earthquakes). The following thesis discusses the research program of testing the response of the interface of a textured GM (GMX) and a GCL. A large dynamic direct shear machine developed by Fox et al. (2006) has been used for the testing process. This machine allows larger specimens and larger normal stresses than for common direct shear devices.

Commonly used geosynthetic materials were carefully chosen from some of the most well-known manufacturers. The GCL was Bentomat DN provided by CETCO (Hoffman Estates, IL). The GMX was a HDPE Microspike/Smooth product produced by Agru America (Georgetown, SC).

The first stage of the testing procedure considered the monotonic (single-direction) shear strength of the GMX/GCL interface. The displacement rates, R, used in this procedure were 1, 100, 10000, and 25000 mm/min. A GCL internal shear strength test was also run

at R = 0.1 mm/min in order to find the shear stress necessary to cause internal failure. The results indicate that displacement rate does not have a large effect on the peak shear strength. All tests reached their peak stress approximately the same displacement. Each test was carried out to a displacement of 200 mm.

The second stage of the testing program considered the cyclic loading response of the GMX/GCL interface. Displacement amplitudes $\Delta_a = \pm 2$, 10, 15, 20, 30, 60, and 120 mm, were applied to seven specimens. These cyclic tests used a sinusoidal wave form with a frequency of 1Hz and a total of 25 cycles. The displacement amplitudes included both pre-peak ($\Delta_a = \pm 2$ and 10 mm) and post-peak ($\Delta_a = \pm 15$, 20, 30, 60, and 120 mm) displacements. The cyclic behavior was analyzed.

The last stage of the research program examined the post-cyclic static shear response of the GMX/GCL interface. Each post-cyclic static test was carried out at a displacement rate of R = 1 mm/min. For $\Delta_a < 15$ mm, the peak shear stress was not affected, and corresponded to the peak shear stress of the monotonic test completed with no previous cyclic testing. For $\Delta_a \geq 15$ mm, the peak strength was greatly reduced. For displacements greater than $\Delta_a = 20$ mm, small peak strength reductions continued until $\Delta_a = 120$ mm. The large-displacement shear strength of the tests that underwent cyclic testing was slightly less than that of the test that did not undergo cyclic testing.

TABLE OF CONTENTS

LIST OF FIGURES

LIST OF TABLES

ACKNOWLEDGEMENTS

This undergraduate Honor's Thesis could not have been completed without the assistance of many people. First, I would like to thank Jason Ross for instructing me on the use of the direct shear machine, and answering any question that I may have had. Also, I would like to thank Dr. Patrick Fox for giving me the opportunity to perform research my senior year. Additional thanks go to Dr. Halil Sezen for serving on my Honor's Defense Committee. This would not have been possible without the support of my parents, or my girlfriend, Lori, for understanding the amount of work that went into this research. Lastly, I would like to thank the College of Engineering for providing a Scholarship to help support my research.

CHAPTER 1

INTRODUCTION AND BACKGROUND INFORMATION

1.1 Introduction

This research provides an analysis of geomembrane/geosynthetic clay liner (GM/CGL) interface response to both monotonic and cyclic shear at 692 kPa normal stress. A geosynthetic clay liner is a manufactured hydraulic barrier bonded to geosynthetic materials (Fox and Stark 2004). GCLs are used in top and bottom liner systems for waste disposal facilities, or landfills. Often, the GCL is used in conjunction with a GM as a composite landfill liner. This composite liner prevents the flow of liquids and gases into and out of the landfills. On the surface of the landfill, the cover system is used to keep out rainfall, where it would generate leachate as it percolated slowly through the waste. Leachate is a toxic liquid created from the mixture of

rainwater with solid waste. The bottom liner system, if installed and working correctly will prevent this leachate from entering the groundwater system. The bottom liner system directs the leachate to a collection sump where it will be removed and treated for contamination (Sura 2009).

The typical landfill liner system consists of many layers and they each serve a different purpose. Figure 1.1 displays a typical composite landfill liner. The top layer is the leachate collection system (LCS) that allows for drainage of the leachate from the top of the GM. This system is typically composed of a pervious material such as gravel or a geocomposite drain (Nye 2007). The next layer is the geomembrane (GM). The GM is essentially impermeable, but due to manufacturing and construction, 3-5 holes per acre can be expected to develop in the GM (Sura 2009). Because of the possibility that leachate will flow through the GM, there is a mineral barrier beneath the GM. This mineral barrier is either a compacted clay liner (CCL) or a GCL. Typical specifications for the CCL include a thickness of 91 cm and a hydraulic conductivity of $1x10^{-7}$ cm/s. In order to limit the thickness of the composite liner, sometimes a GCL is used in place of the CCL. The GCL is typically less than 1 cm thick depending on normal stress and has a specified maximum hydraulic conductivity of $1x10^{-9}$ cm/s (Fox and Stark 2004).

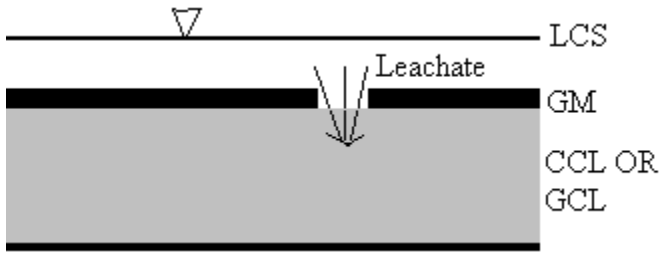

Figure 1.1 Typical landfill liner system.

In many applications, these liner systems need to be placed on slopes, and therefore, stability is a critical part of the design. This research focuses on the interface shear strength developed between the GM and GCL. Aside from a possibility of liner failure due to construction on a slope, liner systems that are installed in seismic regions also pose a threat of failure due to movements caused by earthquake activity (Nye 2007). These two failure modes are the basis for this research.

1.2 Material Selection

There are many different geosynthetic materials manufactured for landfill liner and cover systems. The focus of this research project will be on two products commonly placed next to one another in a composite landfill liner. These two liner system components are the GM and the GCL. A GCL generally consists of a two geotextiles (GTs) encompassing a layer of bentonite. A GCL can be reinforced or unreinforced. Unreinforced GCLs contain no geosynthetic reinforcement across the bentonite layer. Hence, the shear strength for unreinforced GCLS is equal to the shear strength of the bentonite (Fox and Stark 2004). Unreinforced GCLs can be GT-supported or GM-supported. For the GT-supported unreinforced GCL the bentonite is contained by either woven (W) or non-woven (NW) GTs and is able to absorb moisture from the surrounding soil. The GM-supported unreinforced GCL encapsulates the bentonite with either a smooth geomembrane (GMS), or a textured geomembrane (GMX). Encapsulating the bentonite between two GMs prevents the bentonite from becoming hydrated and

therefore, it maintains higher shear strength (Fox and Stark 2004). Reinforced GCLs are GT-supported and can be either stitch-bonded (SB) or needle punched (NP).

The SB GCLs have parallel lines of stitching that run in the machine direction. These lines of stitching allow shear stress to be transferred across the bentonite layer, and provide a much higher shear strength. NP GCLs have fibers that extend from a NW GT through the bentonite and are anchored in a W or NW GT layer. The resulting reinforced GCL product is either a W/NW or NW/NW NP GCL. (Fox and Stark 2004)

Previous research in this area has been completed on many different interfaces. Many testing programs are needed because there are many possible interfaces in a landfill, and many possible combinations of geosynthetic products manufactured. Some past research studies that focused on similar topics as this research study are presented in Chapter 2.

In this research program, a GM/GCL interface is tested in monotonic and cyclic shear. The GCL was a NW/NW NP GCL, Bentomat DN manufactured by CETCO (Hoffman Estates, IL). The NW/NW NP GCL is commonly used when a GCL/GM interface is present. The exact specifications for this product, as provided by the manufacturer, are shown in Figure 1.2. The GM used in this program was a high density polyethylene (HDPE) Microspike/Smooth GMX manufactured by Agru America (Georgetown, SC). The exact specifications for this product are shwon in Figure 1.3.

MATERIAL PROPERTY	TEST METHOD	TEST FREQUENCY $ft^2(m^2)$	REQUIRED VALUES
Bentonite Swell Index[1]	ASTM D 5890	1 per 50 tonnes	24 mL/2g min.
Bentonite Fluid Loss[1]	ASTM D 5891	1 per 50 tonnes	18 mL max.
Bentonite Mass/Area[2]	ASTM D 5993	40,000 ft^2 (4,000 m^2)	0.75 lb/ft^2 (3.6 kg/m^2) min
GCL Grab Strength[3]	ASTM D 6768	200,000 ft^2 (20,000 m^2)	50 lbs/in (88 N/cm) MARV
GCL Peel Strength[3]	ASTM D 6496	40,000 ft^2 (4,000 m^2)	3.5 lbs/in (6.1 N/cm) min
GCL Index Flux[4]	ASTM D 5887	Weekly	1 x 10^{-8} m^3/m^2/sec max
GCL Hydraulic Conductivity[4]	ASTM D 5887	Weekly	5 x 10^{-9} cm/sec max
GCL Hydrated Internal Shear Strength[5]	ASTM D 5321 ASTM D 6243	Periodic	500 psf (24 kPa) typ @ 200 psf

Figure 1.2: Material properties for Bentomat DN GCL (CETCO TR-401 BMDN, 2007).

Property	Test Method	Values		
Thickness, nominal (mm)		60 (1.5)	80 (2.0)	100 (2.5)
Thickness (min. ave.), mil (mm)	ASTM D5994*	57 (1.43)	76 (1.90)	95 (2.38)
Thickness (lowest indiv. for 8 of 10 spec.), mil (mm)	ASTM D5994*	54 (1.35)	72 (1.80)	90 (2.25)
Thickness (lowest indiv. for 1 of 10 spec.), mil (mm)	ASTM D5994*	51 (1.28)	68 (1.70)	85 (2.13)
*The thickness values may be changed due to project specifications (i.e., absolute minimum thickness)				
Asperity Height (min. ave.), mil (mm)	GRI GM12	16 (.41)	16 (.41)	16 (.41)
Density, g/cc., minimum	ASTM D792, Method B	0.94	0.94	0.94
Tensile Properties (ave. both directions)	ASTM D6693, Type IV			
Strength @ Yield (min. ave.), lb/in width (N/mm)	2 in/minute	132 (23.1)	176 (30.8)	220 (38.5)
Elongation @ Yield (min. ave.), % (GL=1.3in)	5 specimens in each direction	13	13	13
Strength @ Break (min. ave.), lb/in width (N/mm)		132 (23.1)	176 (30.8)	220 (38.5)
Elongation @ Break (min. ave.), % (GL=2.0in)		350	350	350
Tear Resistance (min. ave.), lbs. (N)	ASTM D1004	45 (200)	60 (267)	72 (320)
Puncture Resistance (min. ave.), lbs. (N)	ASTM D4833	120 (534)	150 (667)	180 (801)
Carbon Black Content (range in %)	ASTM D4218	2 - 3	2 - 3	2 - 3
Carbon Black Dispersion (Category)	ASTM D5596	Only near spherical agglomerates for 10 views: 9 views in Cat. 1 or 2, and 1 view in Cat. 3		
Stress Crack Resistance (Single Point NCTL), hours	ASTM D5397, Appendix	300	300	300
Oxidative Induction Time, minutes	ASTM D3895, 200°C, 1 atm O_2	≥100	≥100	≥100
Melt Flow Index, g/10 minutes	ASTM D1238, 190°C, 2.16kg	≤1.0	≤1.0	≤1.0
Oven Aging	ASTM D5721	80	80	80
with HP OIT, (% retained after 90 days)	ASTM D5885, 150°C, 500psi O_2			
UV Resistance	GRI GM11	20hr. Cycle @ 75°C/4 hr. dark condensation @ 60°C		
with HP OIT, (% retained after 1600 hours)	ASTM D5885, 150°C, 500psi O_2	50	50	50
These product specifications meet or exceed GRI's GM13				

Figure 1.3: Product information for HDPE Microspike/Smooth GMX (Agru America 2007).

1.3 Overview of Research

This research project was designed to determine the effect of dynamic loading on GCL shear response. As mentioned previously, these liner systems are often placed in seismic regions and the results of this research will help to better understand how the GM/GCL interface will react under earthquake loading. Tests were performed for a singlenormal stress of 692 kPa, which would be a reasonable loading of a bottom liner system in an average landfill. This represents approximately 52 m of municipal solid waste. Although there has been research completed on the dynamic response of GCLs, the majority of these tests have been completed on small specimens at low normal stresses, and lack in shear machine capabilities (Lai et al. 1998, LoGrasso et al. 2002, Kim et al. 2005). The results of the research will better help landfill designers understand the effects of earthquake loading on the GM/GCL interface, and thus allow for more efficient designs.

Although the focus of this research will be determining the effect of dynamic loading on shear response of the GM/GCL interface, it is important to first gain an understanding of the monotonic response at constant displacement rate. A baseline displacement rate of 1 mm/min is the current ASTM standard displacement rate for interface testing of geosynthetics (Fox and Stark 2004). All of the tests that were completed were displacement-controlled, opposed to stress-controlled and, as such, post-peak strength reduction could be easily determined for each test. The peak shear strength, τ_p, and large-displacement shear strength, τ_{ld}, were measured for all monotonic tests. Displacements of 200 mm were reached in all monotonic tests, but displacements

between 500-750 mm are likely needed for residual shear strengths in interface testing (Stark et al. 1996).

The second area of focus for this study is the response of the GM/GCL interface to cyclic loading. Cyclic shear tests were completed to a total of 25 cycles, at a frequency of 1 Hz and for displacement amplitudes ranging from 2 to 120 mm. Each cyclic shear test was followed by static shear at 1 mm/min to measure the post-cyclic static shear strength. According to Nye and Fox (2007), the waveform and frequency have minimal effects on observed behavior of a GCL internal shear strength test. It is also expected that changing frequency and waveform will have little effect for interface behavior.

Chapter 2 of this thesis presents a literature review on the topic of GCL shear strength. Chapter 3 gives a detailed description of the test procedures that were followed. Chapter 4 presents the test data that was collected. Overall conclusions of the research are presented in Chapter 5. All test results not included in the body of the thesis can be found in the Appendix.

CHAPTER 2

LITERATURE REVIEW

2.1 Introduction

GCLs have been extensively studied in the past, but with the continual advancements of products and testing procedures, there is always a need for more research. Project specific testing is always recommended when using geosynthetic products in landfill liner systems. However, research programs can provide behavioral tendencies of the geosynthetics that can provide insight into expected interactions on the interface. Although many of the articles delve much deeper into the subject matter than will be discussed herein, an overview of the general state of knowledge for GCL shear testing and shear strength is presented in Chapter 2.

2.2 State-of-the-art report: GCL shear strength and its measurement (Fox and Stark 2004)

This publication presents a comprehensive source of information on the shear strength and shear testing of GCLs. This paper is very informative for this research because it summarizes the state of the GCL shear testing up to the date of publication. Many of the procedures used in this research are discussed from this paper, and the highlights will be provided below.

The first important section of this paper discusses the shear stress-displacement relationships for GCLs and GCL interfaces. Figure 2.1 displays a typical shear stress vs. displacement curve for an internal shear test of a hydrated GCL. In general it was found that the shear displacement corresponding to peak strength, Δ_p, was less than 50 mm. The peak displacement is smallest for unreinforced GCLs, larger for NP GCLS, and largest for SB GLCs. All GCLs and most GCL interfaces experience a large post-peak strength reduction as displacement continues and ultimately reach a residual shear strength τ_r. After this point, no further strength reduction occurs. This post peak strength reduction can be attributed to clay particle reorientation at the failure surface, volume increase of material within the shear zone, loss of roughness for geosynthetic materials (e.g. GMX), or failure of reinforcement or supporting geotextiles (GTs). The residual strength ratio, τ_r/τ_p for internal GCL shear tests vary greatly with values ranging from 0.04 to 1. In general, the ratio for GCLs increases in the following order: hydrated NP GCL< hydrated SB GCL< hydrated unreinforced GCL< dry unreinforced GMS supported GCL (Chiu and Fox 2004; Fox et al. 1998)

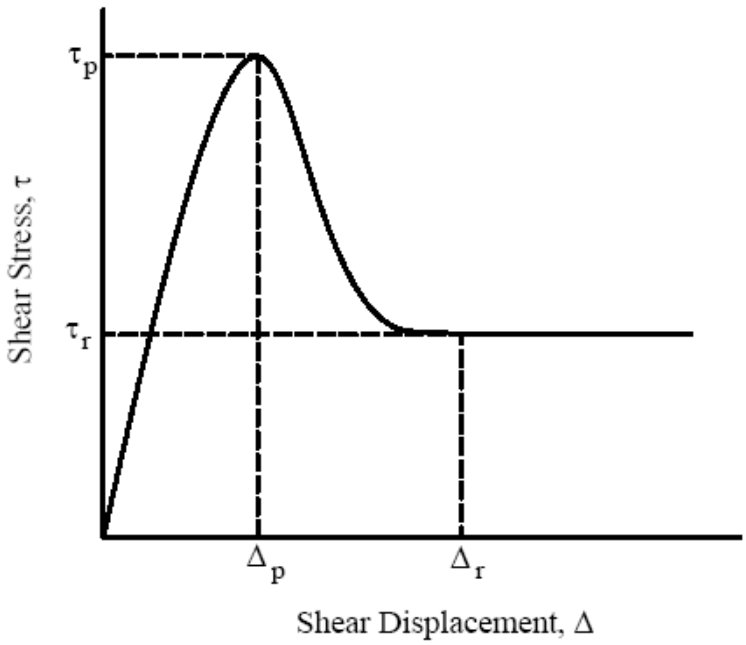

Figure 2.1: Typical shear stress-displacement curve for a static shear test (Fox and Stark, 2004).

An important consideration for designers is the development of failure envelopes from shear test data. The failure envelopes are prepared by plotting shear strength versus total shearing normal stress. Figure 2.2 displays typical failure envelopes for GCLs and GCL interfaces. In general the internal peak strength failure envelopes for GCLs are often non-linear, where peak strength failure envelopes for GCL interfaces can be linear, multi-linear, or bi-linear. Failure envelopes that pass through the origin are typical of both GCL interface and internal shear strength of unreinforced GCLs. For a reinforced GCL, it is difficult to determine if there is a zero cohesion intercept ($c = 0$) because of difficulties with an adequate gripping surface at low normal stresses. The Mohr-Coulomb failure criterion is used to develop a failure envelope, using two parameters, cohesion

intercept, c, and friction angle, φ. The determination of these two values can only be completed by laboratory testing (Fox and Stark 2004, Stark et al. 2000).

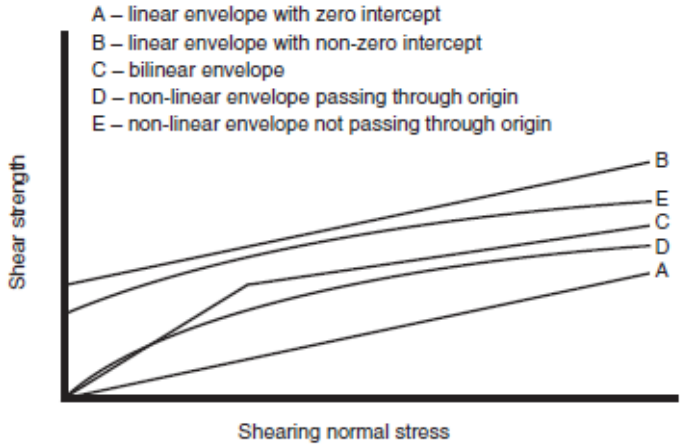

Figure 2.2 Typical failure envelopes for GCLs and GCL interfaces (Fox and Stark 2004).

The authors also discuss the importance of long term testing. The majority of data that is obtained from GCL testing is short term shear strength data, yet, GCLs are expected to sustain loads for hundreds of years. The justification for using the short term testing is that the short term shear strength data is relevant to long term stability of GCLs. A problem with making this assumption is that GCL creep and GCL durability cannot be predicted using short term shear tests. The definition of creep is continuing shear displacement under constant normal and shear stress conditions. The applied shear stress divided by the short-term peak shear strength at the same normal stress is the creep stress ratio. The biggest issue with creep concerning GCLs is that creep failure may occur at a stress ratio less than 1 due to reinforcement fibers that elongate, break, or pull-out of the supporting GTs over time. Although there has been relatively few creep tests performed

on GCLs because of the difficulty and time required, it is still important to remember that the possibility for creep is a real concern when designing a waste disposal facility. Creep is an issue where continuing research is needed. Another issue with short-term testing is that it does not measure the durability, or how the GCL reinforcement fibers degrade over time. Aging and creep are interrelated processes that occur simultaneously over the lifetime of the GCLs (Fox and Stark 2004). The durability of the GCL is also something that is not included in this present research, but it is something that must be considered in design.

ASTM D 6243 is the current standard test method for the measurement of internal and interface shear strength test of GCLs in the United States. The requirements of this standard include: GCLs be tested in direct shear with a minimum specimen dimension of 300 mm, and the test specimen is sheared between two shearing blocks, each of which is covered with a gripping surface that transfers shear stress to the specimen. For displacement controlled tests, ASTM D 6243 recommends Equation 2.1 to determine the maximum shear displacement rate:

$$R = \frac{\Delta_f}{50\, t_{50}\eta} \tag{2.1}$$

where Δ_f is the estimated displacement at peak or large-displacement shear strength, t_{50}, - is the time required for the GCL specimen to reach 50% consolidation, and η = 1 for internal shear of GCL, η = 4 for interface shear between a GCL and an impermeable material, and η = 0.002 for interface shear between a GCL and a permeable material. It was found that this equation could lead to shearing rates as low as 0.001 - 0.0001

mm/min which would make tests run for 34.7 and 347 days respectively for a displacement of 50 mm. If shearing pore pressures are not expected on a GCL interface, for static shear R = 1 mm/min is recommended, which is the rate that was chosen for the present research for static shear. After the test has been completed, a minimum of 5 water content samples should be taken from the specimen to ensure that uniform hydration has occurred.

In this paper, many testing machines are described that are capable of performing shear testing on GCLs. They include direct shear machine, torsional ring shear, and inclined plane shear. The most advantageous machine is the direct shear because it measures shear in one direction and produces uniform shear displacement. Torsional ring shear has the advantage that it can provide unlimited shear displacement and thus can obtain residual shear strength, τ_r not just large-displacement shear strength, τ_{ld}. The inclined plane shear device has been used in Europe, but few results have been reported for this device. For the present research a large dynamic direct shear machine is used.

The paper by Fox and Stark (2004) also discusses the importance of proper GCL hydration. The hydration method that was used in the present research was first developed in Fox et al. (1998) but is also presented in this paper. In the past, it was customary to leave the specimen in the testing chamber of a shear machine for 10-20 days so it would reach the proper water content for testing. The shear strengths of GCLs and GCL interfaces are affected by the hydration procedure and the hydration liquid. The water content of the GCL specimen should be comparable to the water content that is expected in the field when a shear test is performed. As far as the proper hydration liquid

to use, tap water is almost always used because it has chemical make-up resembling that of the pore water in most soils. Under ideal conditions, the GCL specimen should be hydrated to equilibrium (no further volume change). This process can take up to three weeks (Gilbert et al. 1996). The incomplete hydration of a GCL may result in the measurement of unconservative shear strengths (i.e. too high). With this in mind, an accelerated two-stage hydration approach was developed. The first step in the 2-stage hydration procedure includes hydrating the GCL under low normal stress (1 kPa) to reach the water content that is expected for the shearing normal stress. At least 24 hours should be allowed for stage 1 hydration. Next, during stage 2, the specimen is placed in the test chamber of a direct shear machine, and the normal stress is immediately applied to the specimen. The specimen is then allowed free access to water for another 24-48 hours. With this two-stage process the time for hydration can be reduced from 10-20 days to 1-3 days. Figure 2.3 displays the shows the volume change data for two W/NW NP GCLs. One specimen was subjected to the two-stage hydration procedure discussed above, and the other was not. It can be observed in the figure that the specimen hydrated using the accelerated specimen reached equilibrium within about 5 hours, where after 50 hours the non-accelerated specimen was still undergoing volume change.

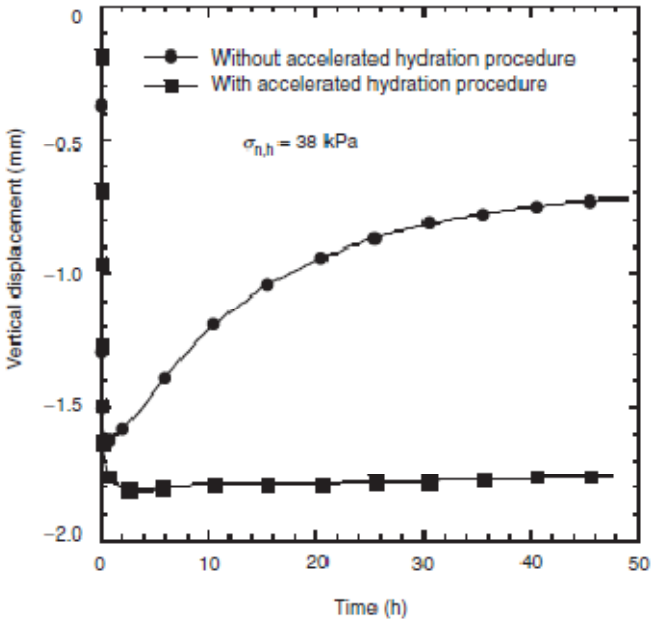

Figure 2.3: Effect of two-stage accelerated hydration procedure for a W/NW NP GCL (Fox et al. 1998).

2.3 Dynamic shear behavior of a needle-punched geosynthetic clay liner (Nye and Fox 2007)

This research program described in this paper was very similar to what was done for the present research. Nye and Fox looked at the cyclic response of a GCL under a single normal stress of 141 kPa. Besides using the cyclic testing parameters described above (sinusoidal wave form, 1 Hz, 25 cycles), this research looked at a number of different parameters to see the effect they had on the results previously obtained. This testing program provided very valuable results, with the most important being summarized below.

The first parameter that was tested was the number of cycles, N. Tests were run at $N = 15$ and $N = 100$, in addition to the standard test at $N = 50$. Figure 2.4 displays post-cyclic shear static strength vs. number of cycles. It can be observed on this plot that after 10 cycles, there is not a significant decrease in peak or residual strength of the GCL.

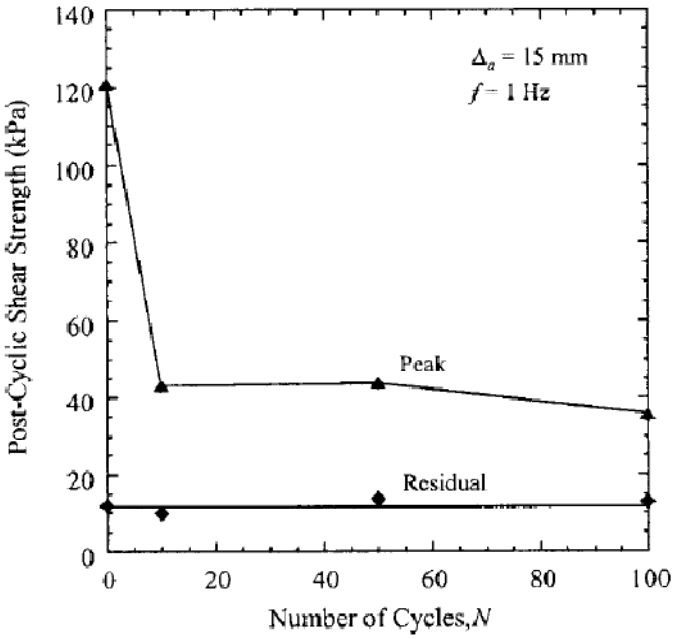

Figure 2.4: Effect of number of cycles on post-cyclic static shear strength (Nye and Fox 2007).

The next parameter that was investigated was cyclic frequency, f. The additional frequencies investigated were $f = 0.1$, 0.5, 2 and 3 Hz ($\Delta_a = \pm 15$ mm and $N = 5$) Figure 2.5 displays the effects of frequency on a plot of maximum shear stress versus number of cycles. It can be observed from this plot that frequency does not have a noticeable effect on the max stress envelope of the GCL. Figure 2.6 displays both peak and residual post-

cyclic static shear strengths. Although there is some scattering, the post cyclic shear strength appears to be unaffected by loading frequency.

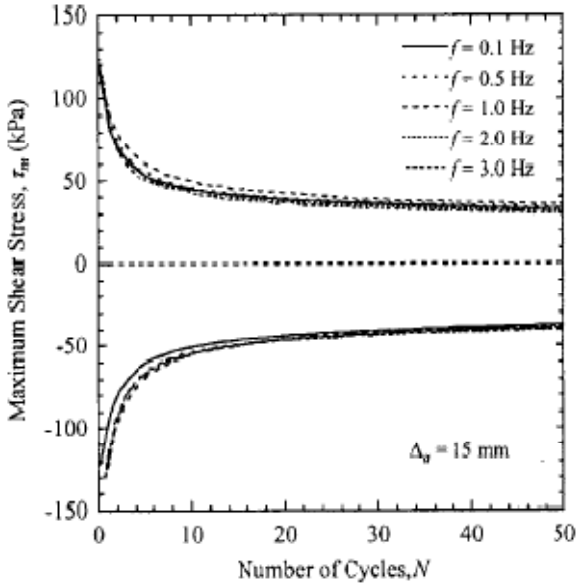

Figure 2.5: Effect of frequency on the shear stress envelope (Nye and Fox 2009).

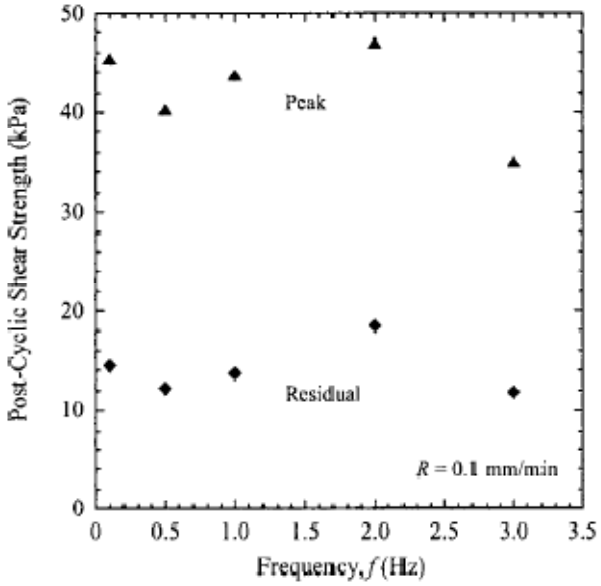

Figure 2.6: Effect of frequency on post-cyclic static shear strength (Nye and Fox 2007).

Finally, the effects of waveform on GCL internal shear strength was investigated. A sinusoidal waveform was used for the original cyclic tests. To determine the effect of changing waveform could have additional tests were conducted using square and triangular waves (Δ_n =15 mm, N = 50). Figure 2.7 displays the maximum shear strength versus number of cycles for all 3 waveforms. It can be observed from this plot that waveform has little effect on the shear stress envelope.

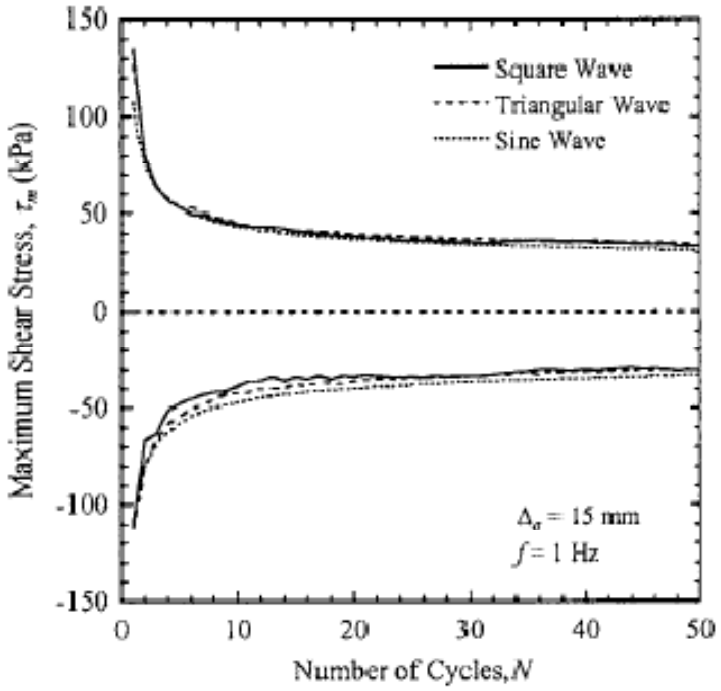

Figure 2.7: Affect of waveform on maximum shear versus number of cycles (Nye and Fox 2007).

A summary of the findings of Nye and Fox (2007) regarding the changing parameters for cyclic testing of GCLs is as follows:

1. Changing the number of cycles does not change the post-cyclic shear strength after N = 10 for GCL internal shear strength.

2. Changing the loading frequency of the cycles does not have an impact on either the shear stress envelope or post-cyclic shear strength of the GCL.
3. The waveform does not have an effect on the post-cyclic shear strength or the shear stress envelope.

All three of these conclusions combine to show that displacement amplitude is the biggest factor in determining the cyclic response in GCL internal shear strength testing as also will be shown with the present research.

2.3 Monotonic and cyclic shear response of a needle-punched geosynthetic clay liner at high normal stresses (Sura 2009)

Sura (2009) investigated internal GCL shear strength at various normal stresses in both monotonic and cyclic shear. The experimenal procedures were very similar to those used in the present research. Sura (2009) used a W/NW NP GCL, Bentomat ST, manufactured by CETCO (Hoffman Estates, IL).

Sura (2009) first describes the monotonic shear testing of the GCL with displacement rates ranging from 0.1 to 25000 mm/min. Many important conclusions can be made from data gathered. Figure 2.8 displays the shear stress-displacement curve for monotonic shear tests at σ_n = 692 kPa, which is the same normal stress used in the current research project. From this plot, it can be observed that both τ_p and τ_r increase with increasing displacement rate. This trend is consistent with past research. A possible exception is at very low rates (Nye and Fox 2007). It can also be observed that there is a "false peak" within the first 5 mm of displacement. This false peak effect represents the

necessary displacement for the teeth of the bottom gripping surface to grip the bottom GT of the GCL specimen. The initial rise in shear strength before the false peak is attributed to frictional resistance, and after the false peak, the rise is the actual measured shear strength of the specimen. This initial frictional resistance is a minor consequence of the gripping method and it does not affect the actual measured performance of the GCL specimen. The failure method did not change in these tests, as internal failure was forced in all cases. Internal failure always occurred between upper W GT and the bentonite layer.

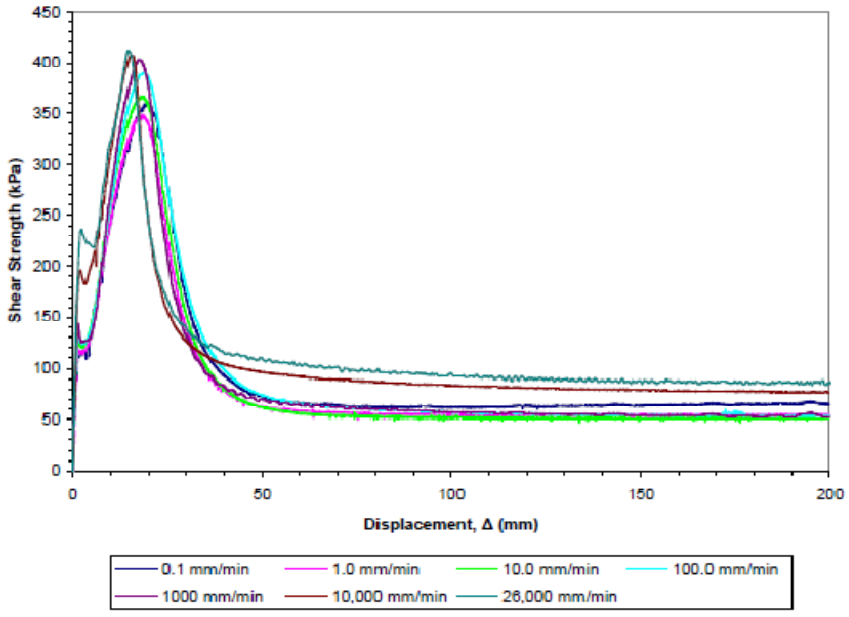

Figure 2.8: Stress-displacement curves for monotonic shear tests at σ_n = 692 kPa (Sura 2009).

Figure 2.9 displays peak shear strengths as a function of displacement rate for monotonic shear tests. This figure includes data for multiple normal stresses, and it can

be observed that increasing normal stress increases the peak strength of the specimen. Across each normal stress, it can be observed that the peak strength first increases with displacement rate until it reaches a maximum and then decreases until the highest displacement rate is reached. As normal stress increases, the variations in peak strength increase. The increasing trend is more prevalent at σ_n = 1382 kPa, but is still present at σ_n = 692 kPa.

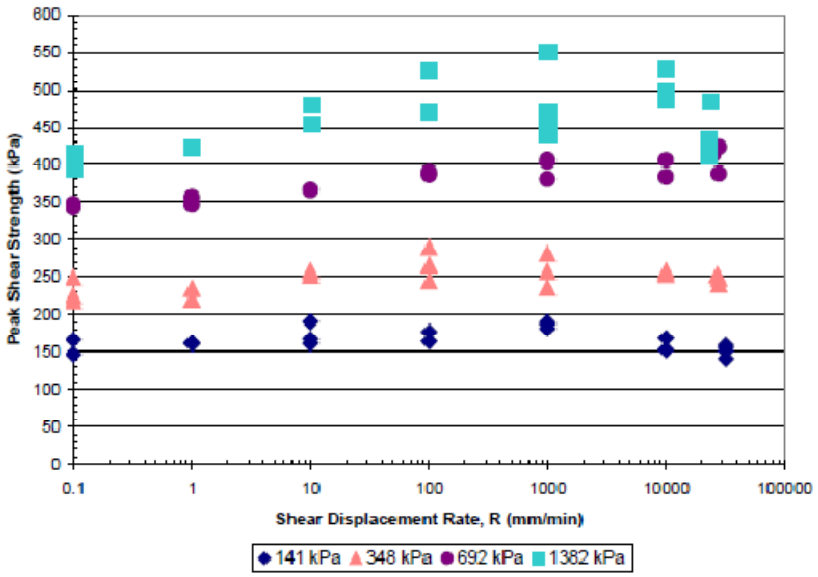

Figure 2.9: Peak strengths as a function of displacement rate for monotonic shear tests (Sura 2009).

Figure 2.10 displays the corresponding residual shear strengths as a function of displacement rate and normal stress. In general it is observed that that the residual shear strength increases with increasing displacement rate and normal stress. The residual strength at a static rate of 0.1 mm/min is larger than the residual strength at 1.0 mm/min. The trend for residual shear strength at σ_n = 692 kPa continues to decrease until a

displacement of 10 mm/min and then increases with increasing displacement rate. This increase agrees with previous literature (Eid et al. 1999, Fox et al. 2004). This effect has been previously attributed to the rate-dependant shear resistance of hydrated bentonite (Fox et al. 1998).

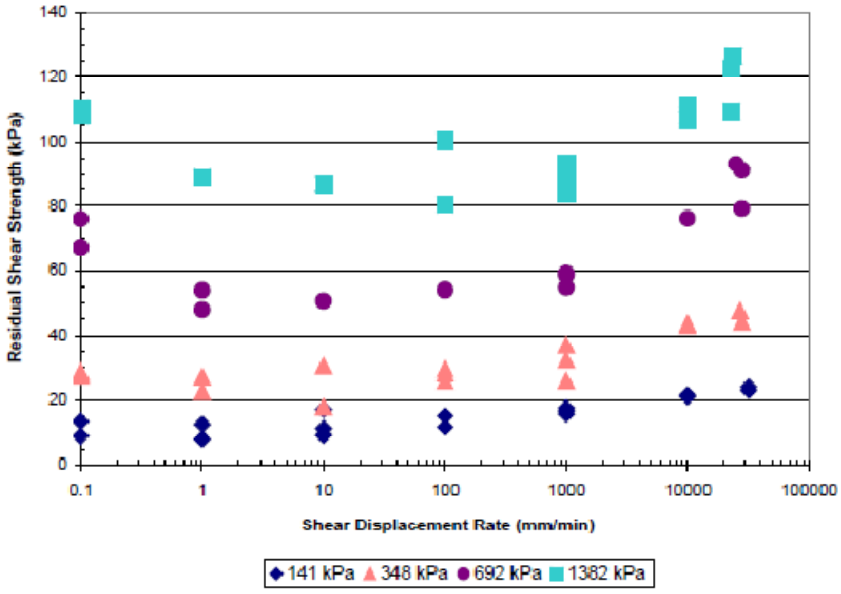

Figure 2.10: Residual shear strengths as a function of displacement rate for monotonic shear tests (Sura 2009).

Sura (2009) also investigated the cyclic testing of the GCL at normal stresses of 348 kPa, 692 kPa, and 1382 kPa. The cyclic tests were performed at a frequency of 1 Hz and a total number of cycles, $N = 50$. After the completion of the cyclic test and rest-period with free access to water, the GCL was subjected to 200 mm of static shear at a displacement rate, $R = 0.1$ mm/min. Figure 2.11 displays a typical shear stress versus time plot during cyclic shear. This figure represents the results of a test with $\sigma_n = 692$ kPa and cyclic displacement amplitude $\Delta_a = 5$ mm. For all normal stresses, the maximum

shear strength was reached on the first cycle, and shear strength decreased with each continuing cycle. Figure 2.12 displays the shear stress-displacement curve for the cyclic test with σ_n = 692 kPa and cyclic displacement amplitude Δ_a = 5 mm. For all cyclic tests, the initial cycle of loading produces the largest shear stress. Following this first cycle, the shear stress continues to decrease until N = 10 where it can be observed that the hysteresis loop starts to repeat itself. This behavior indicates that the majority of the damage of the damage is done to the GCL within the first 10 cycles, and the decline in stress is very gradual after this point.

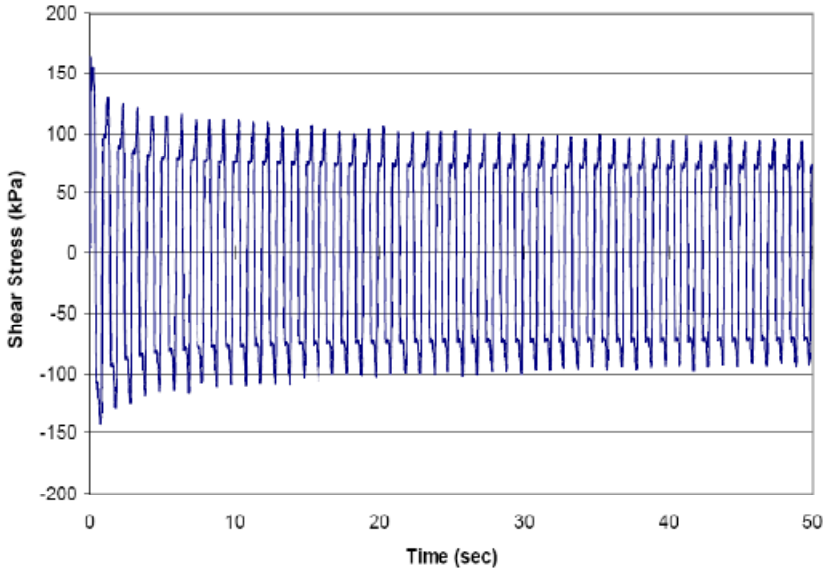

Figure 2.11: Shear stress as a function of time for Δ_a = 5 mm at σ_n = 692 kPa (Sura 2009).

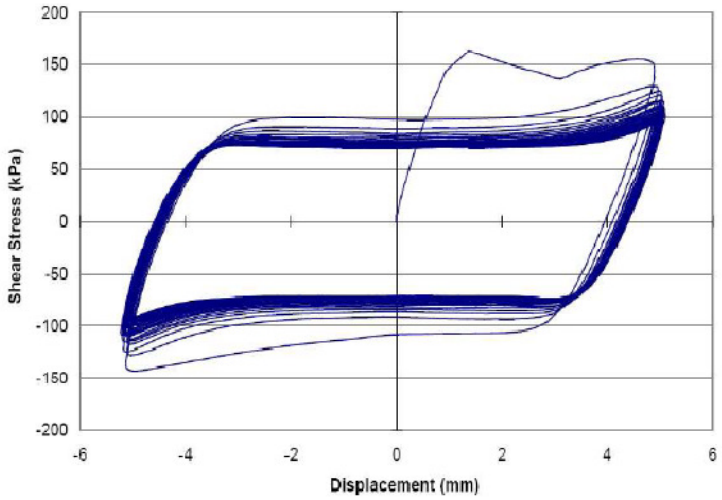

Figure 2.12: Shear stress as a function of displacement during cyclic shear of Δ_a = 5 mm and σ_n = 692 kPa (Sura 2009).

Several dynamic shear response parameters were determined by Sura (2009), including secant shear stiffness, K, and damping ratio, β. The secant shear stiffness is defined in Equation 2.2, where $\tau_{m,1}$ = maximum shear stress for the first half-cycle and $\tau_{m,2}$ = maximum shear stress for the second half cycle. The damping ratio is defined in Equation 2.3, where β_1 and β_2 are the damping ratios of the first and second half-cycles, respectively. A is the total area of the loop, and A_1 and A_2 are the areas displayed in Figure 2.13. Figure 2.13 displays the parameters of equation 2.2 and 2.3 on a hysteresis loop. This loop is typical of what is to be expected for a cyclic GCL internal shear test.

$$K = \frac{K_1 + K_2}{2} = \frac{\tau_{m,1} + \tau_{m,2}}{2\,\Delta_a} \tag{2.2}$$

$$\beta = \frac{\beta_1 + \beta_2}{2} = \frac{\frac{A}{4\pi A_1} + \frac{A}{4\pi A_2}}{2} = \frac{A}{4\pi\Delta_a}\left(\frac{1}{\tau_{m,1}} + \frac{1}{\tau_{m,2}}\right) \tag{2.3}$$

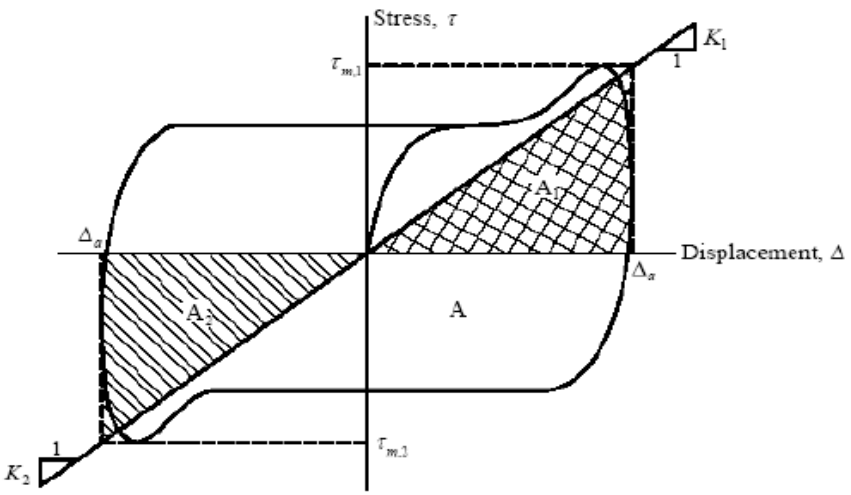

Figure 2.13: Calculation of secant shear stiffness *K* and damping ratio β from hysteresis loop (Nye and Fox 2007).

The plot of K as a function of displacement amplitude for σ_n = 692 kPa is provided in Figure 2.14. It can be observed from the plot that K decreases with increasing number of cycles, *N* and increasing displacement amplitude, Δ_a. Also, it is clear that the displacement amplitude has a larger effect on shear stiffness reduction than *N*.

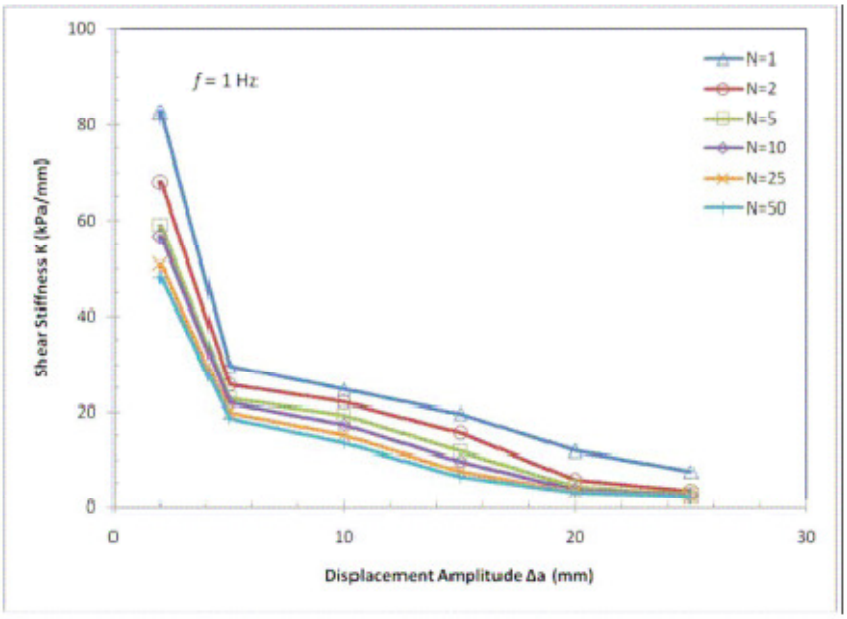

Figure 2.14: Shear stiffness reduction curve at σ_n = 692 kPa.

Figure 2.15 provides the damping ratio versus displacement amplitude according to the number of cycles, *N*. The minimum damping ratio is observed to be between displacement amplitudes (Δ_a) of 10 to 20 mm. In general Sura (2009) found a decreasing and then increasing trend in β as displacement amplitude increases.

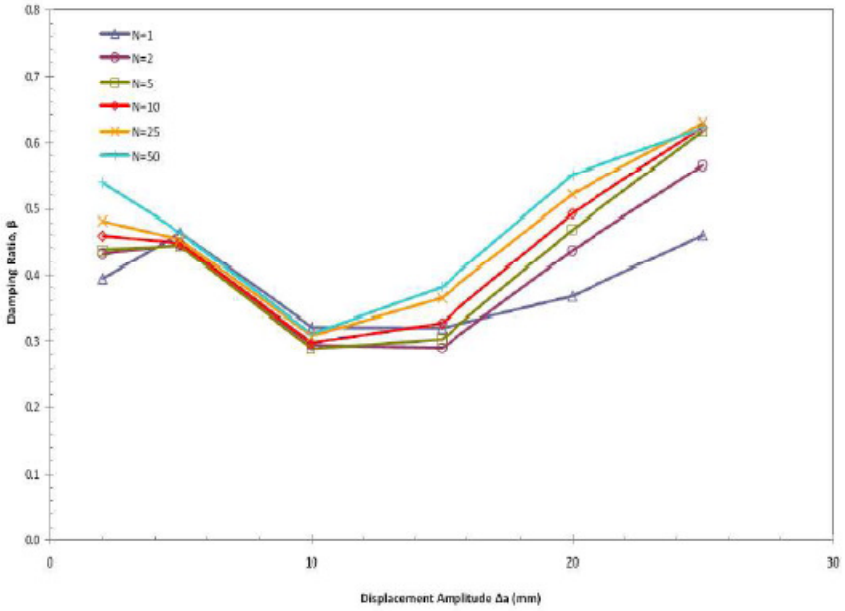

Figure 2.15: Damping ratio as a function of displacement amplitude at σ_n = 692 kPa (Sura 2009).

There are many important conclusions that were made in this thesis that provide strong background knowledge for understanding the behavior of internal dynamic shear behavior of NP GCL's. For the monotonic testing the normal stress was the primary factor in determining the monotonic peak shear strength. The peak strength increases with increasing shear displacement rate, R, until reaching a peak at approximately R = 1000 mm/min and then decreasing until reaching the maximum displacement rate. The static rate, R = 0.1 mm/min, was conservative for all normal stress levels. For cyclic testing, the GCL specimens exhibit the highest strength during the first cycle which then decreases until reaching a repeating hysteresis loop. Peak shear strengths increase with increasing displacement amplitude until Δ_a = 15mm when the strengths no longer are affected by increasing the displacement amplitude, as all of the reinforcement has been damaged during the first cycle of shear.

2.5 Shear strength of HDPE geomembrane/geosynthetic clay liner interfaces (Triplet and Fox 2001)

The papers that have been discussed previously have all dealt with internal failures of GCLs, under both static and cyclic shear loadings. Triplett and Fox (2001) deals with the shear strength of HDPE GM/GCL interfaces under normal stresses ranging from 1 to 486 kPa. In this paper six different GM/GCL interfaces were tested, and these are shown in table 2.1. The interfaces that will discussed with the greatest interest are the CX/NW, and LM/NW because these interfaces most closely represent the materials used in the present research. The CX/NM interface is composed of a round-eye coextruded (CX) textured HDPE geomembrane manufactured by GSE Lining Technology, Inc. (Houston, TX) and a non-woven needle-punched polypropylene geotextile manufactured by Bentomat. The LM GM had texturing that was laminated onto a 1.0 mm smooth backing GM.

TABLE 1. GM/GCL Interfaces Tested for Experimental Program

GM/GCL interface	Geomembrane	Geosynthetic clay liner
SM/W	Smooth HDPE (40 mil)	Woven geotextile of woven/ nonwoven needle-punched GCL
SM/NW	Smooth HDPE (40 mil)	Nonwoven geotextile of woven/nonwoven needle-punched GCL
LM/W	Laminated textured HDPE (40 mil)	Woven geotextile of woven/ nonwoven needle-punched GCL
LM/NW	Laminated textured HDPE (40 mil)	Nonwoven geotextile of woven/nonwoven needle-punched GCL
CX/W	Coextruded textured HDPE (40 mil)	Woven geotextile of woven/ nonwoven needle-punched GCL
CX/NW	Coextruded textured HDPE (40 mil)	Nonwoven geotextile of woven/nonwoven needle-punched GCL

Table 2.1: GM/GCL interfaces tested for experimental program (Triplett and Fox 2001).

The specimens underwent direct shear tests to measure the peak shear strength and the large displacement (200 mm) shear strength. Figure 2.12 shows the shear stress vs. horizontal displacement for the (a) LM/NW and (b) CX/NW interfaces. Many impor-

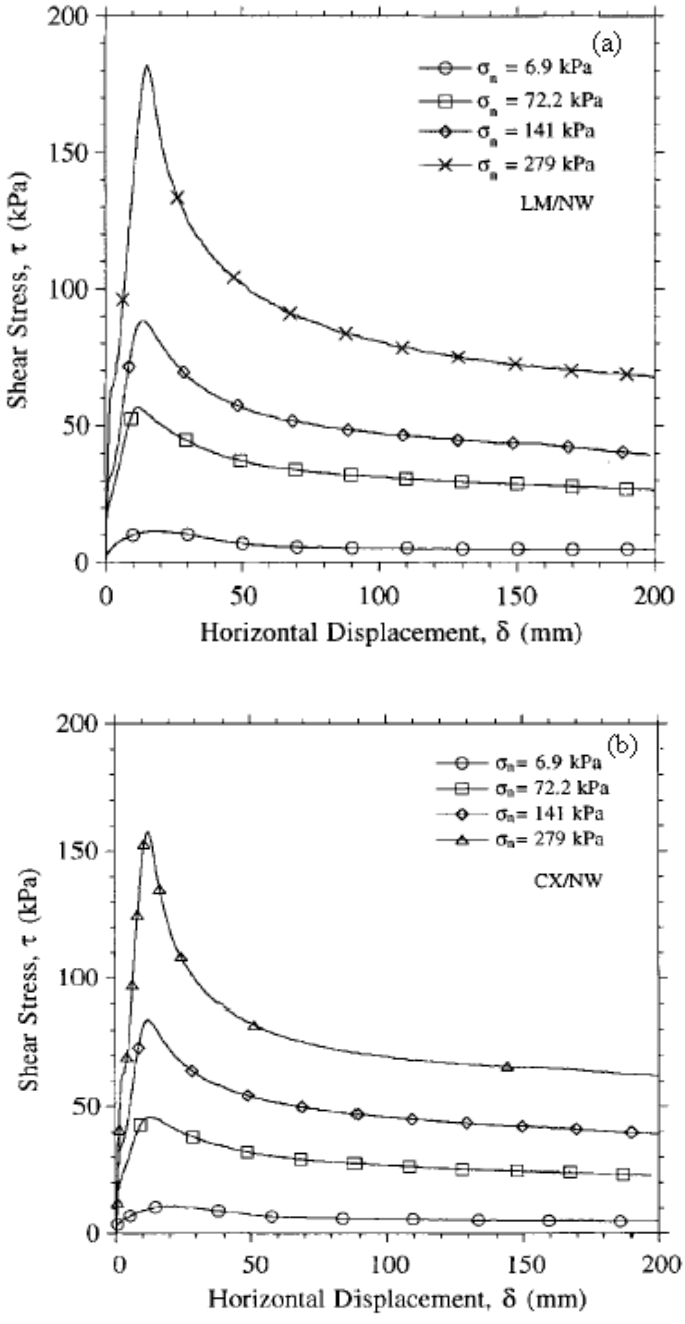

Figure 2.16: Stress-displacement curves for: (a) LM/NW; (b) CX/NW.

tant trends can be seen from these plots. The peak strength of the interface increases with increasing normal stress, and peak strength occurs at very similar displacements. Most curves display large postpeak strength reduction from peak shear strength to large displacement shear strength at δ = 200 mm. Figure 2.12 shows the displacement strength ratio (τ_{ld}/τ_p) vs. normal stress. From this plot, it is observed that displacement ratio is below 0.5 for all tests, indicating a large strength reduction after peak strength.

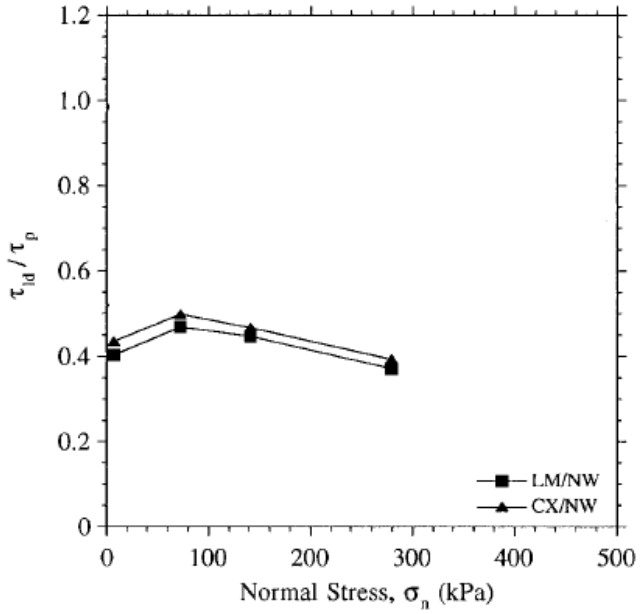

Figure 2.17: τ_{ld}/τ_p for GM/GCL interfaces (Triplett and Fox 2001).

The effect of displacement rate on peak strength and large displacement strength was also tested. The results indicate that there is no consistent trend between displacement rate and measured shear strength which agrees with previously data that indicates the shear strength of a textured GM/NW GT interface is independent of displacement rate (Stark et al. 1996). The most important conclusions reached from this testing program are included below:

1. Long periods of hydration and very slow shearing rates are not needed for GM/GCL interface tests. The two-stage hydration process described previously proves adequate.
2. The failure surface for all tests, with normal stress ranging from 1 to 486 kPa, was located at the GM/GCL interface.
3. All tests experienced post peak reduction with the largest reductions occurring at the largest normal stresses. The displacement where peak strength occurred was similar for the CX/GCL and LM/GCL interface tests.
4. The displacement rate does not seem to have a large effect on peak strength or large displacement strength.
5. The quantity of bentonite extruded at the interfaces increased with increasing normal stresses.

CHAPTER 3

TESTING PROCEDURE

3.1 Introduction to Testing Procedure

A consistent testing procedure was used for all monotonic and cyclic tests, respectively. The methods that were implemented will be described in the following sections. A detailed outline of the methods was provided by Nye (2007). Each test involved a multi-step process. It started with cutting the specimens from a large roll, cutting the individual specimen to fit appropriately in the machine, a two-stage hydration process, followed by testing of the specimen. The equipment and test procedures will be discussed in the following section.

3.2 Testing Machine Description.

The shear machine used in this testing program was a large-scale direct shear machine that is capable of both static and dynamic loading. Fox et al. (2006) provides a detailed overview of the machine, and only the highlights of the machine will be discussed in this section. Figure 3.1 provides a scaled drawing of the machine. One of the major advantages of this machine is that it is able to support very high normal stress.

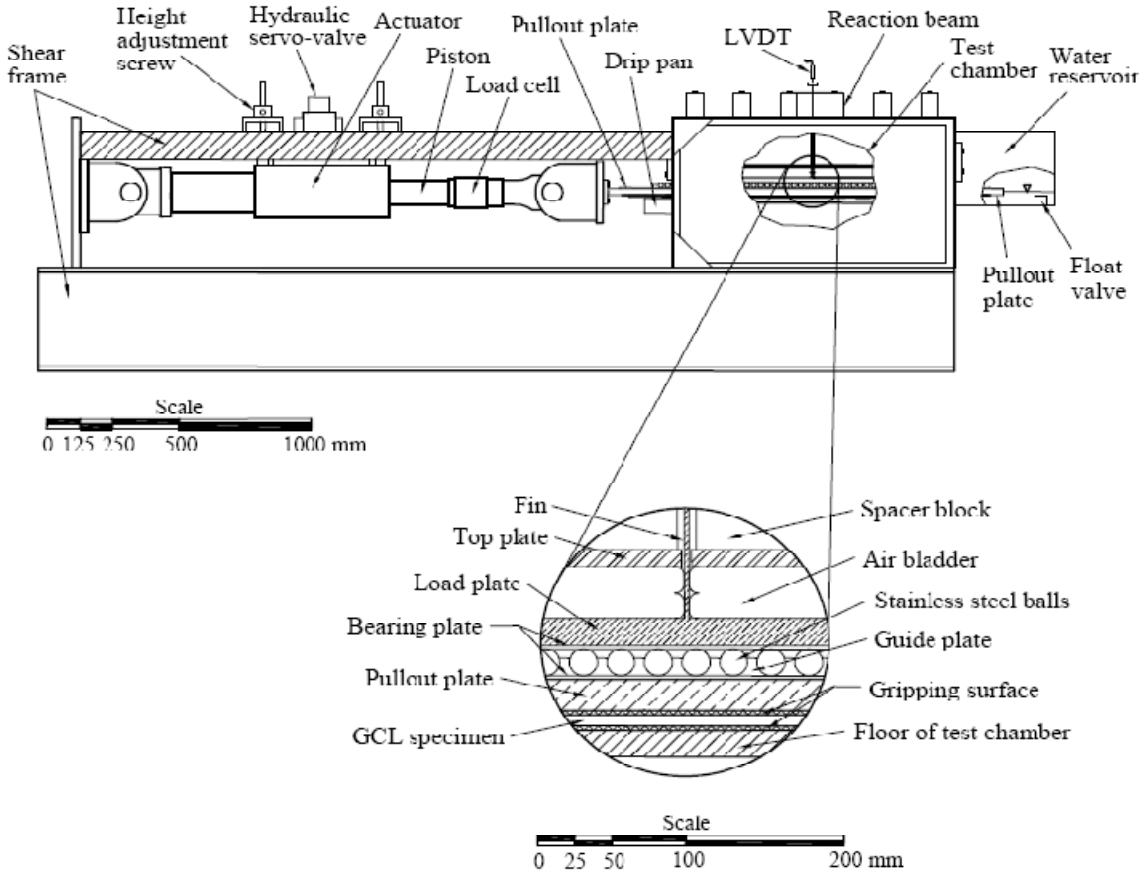

Figure 3.1: Large dynamic direct shear machine (Nye and Fox 2007).

As mentioned previously, there has not been much research performed with large normal stresses, and this machine is able to accommodate normal stresses of 2000 kPa. Another advantage of this machine is that it is capable of shearing a specimen 254 mm, which helps to ensure that large-displacement, τ_{ld} or residual shear strengths, τ_r will be reached. Standard 300 x 300 mm direct shear devices generally do not allow sufficient travel to measure internal residual shear strengths of reinforced GCLs (Fox et al. 1997). Another feature of this device that makes it superior to a standard shear machine is the large specimen size (305 x 1067 mm). The machine is capable of bi-directional movement (i.e., back and forth), and has negligible machine friction. The GCL specimen is sheared between an upper pullout plate, and the floor of the test chamber. The floor of the test chamber has an aggressive gripping surface (modified truss plates). For the interface testing program implemented here, the top gripping surface is a GMX glued to the upper pullout plate. Both ends of the testing chamber are open to allow drainage and hydration. The shearing system is powered by a 245 kN hydraulic actuator. The components of the enlarged test chamber in Figure 3.1 are as follows: floor of the test chamber, GCL specimen, GMX attached to upper pull-out plate with adhesive, a bearing plate, 517 stainless steel balls that reduce the shear stress due to friction to 0.27% of the applied normal stress, another bearing plate, an upper load plate, two bellowed air bladders that provide the normal stress, a top plate, and spacer blocks.

On top of these components are the reaction beams with a linear variable differential transformer (LVDT) attached that measures the volume change before, during, and after testing. All of the information that is collected during the testing procedure is automatically saved to a Dell desktop computer. A software system provided by MTS

delivers instructions to the actuator. Microsoft Excel is used to interpret and store the data (Nye 2007). Nye (2007) includes a detailed outline of all the components of the MTS software that was used, and also explains the use of the software for any given testing procedure from the very beginning of the hydration process to extraction of the data files to Excel.

3.3 Pre-Testing Procedure

The procedures that were followed for this research are ones that have been followed by many past researchers at OSU and have been extensively outlined in reports, such as Nye and Fox (2007). The GCL specimen was cut parallel to the factory roll direction. Each specimen was cut to a size of 1320 x 305 mm. This allows the extra GCL to be pulled into the machine during shear if an internal GCL failure occurs. The specimen was then placed in a hydration pan under a normal stress of approximately 1 kPa for at least 24 hours. This was the beginning of the two-stage hydration procedure that was originally developed by Fox et al. (1998) and was implemented in this testing program. The GCL specimens were hydrated to an initial water content of 80%, as this was the expected final water content of the GCL after hydration at σ_n = 692 kPa. The specimen was then placed into the shear machine, and loaded with the components described in Section 3.2. The required normal stress was applied (σ_n = 692 kPa) to the test specimen, and free access to water was supplied through the hydration system of the shear machine. The machine is designed so water may get to all areas of the specimen to ensure that a proper level of hydration is reached. The specimen is then allowed to

hydrate for another 24 hours under the applied normal stress, completing the second stage of hydration. At this point, the specimen is ready for monotonic or cyclic testing.

3.4 Monotonic Testing Procedure

After the specimen has been properly hydrated, monotonic testing can now take place. The actuator piston is attached to the upper pullout plate via screws. The rate at which the piston moves is controlled by the MTS program mentioned earlier which is run on the Dell computer. From this program every aspect of the testing procedure can be controlled, from the rate to which the piston moves, to how fast data points are collected. After the piston is connected to the upper pull-out plate, and the appropriate tests parameters are set, the test can be started. For this research, a monotonic test is one done with $R > 1$ mm/min, and a static test is one done with $R \leq 1$ mm/min. The displacement rates that were used were R = 0.1, 1, 10, 100, 10000, 25000 mm/min. The R = 0.1 mm/min test was done to induce internal failure and the GMX was replaced by an upper pull-out plate equipped with gripping teeth. The specimens were no longer swelling or contracting at the time of testing. It is important that equilibrium has been reached because if pore pressures accumulate on the shearing interface, the shear strength results will not provide accurate data (Fox and Stark 2004).

3.5 Cyclic Testing Procedure

After the second stage hydration is complete, and the hydration curve has flattened out, indicating equilibrium has been reached, the cyclic process can begin. For

each cyclic test, a sinusoidal wave was imposed on the interface with a frequency of 1 Hz for a total of 25 cycles. The parameter that changed for each test was the displacement amplitude, Δ_a, which ranged from 2 to 120 mm. After the cyclic stage of the test is run, the specimen is then permitted to rest for at least 24 hours at the same normal stress and with t he full access to water. After this rest period, a static shear test is run on the specimen with a displacement rate of 1 mm/min, which is the ASTM standard for interface testing of geosynthetics.

3.6 Post-Testing Procedure

After the monotonic or dynamic testing, the same procedure is followed for specimen removal. First the machine is disassembled and the specimen is removed from the testing chamber. The method of failure is noted, as this can be interface or internal failure for the GM/GCL interface shear tests. Five equal-sized samples are cut from the GCL specimen to obtain the water content of the immediately after testing. The test results are then converted to an Excel worksheet, where they are analyzed, and appropriate plots are created.

CHAPTER 4

TEST DATA

4.1 Introduction

This chapter presents test data from the research program. The first section presents the results of the monotonic shear tests. These tests are important because they provide a standard to compare the post-cyclic shear strength data. The GM/GCL interface has been tested in static shear previously, and this will allow our test materials to be compared to past data. The second section presents the data and plots from the cyclic testing program. Included in this section are the strength parameters that were determined from the cyclic data. The third section of this chapter deals with the post cyclic static shear tests.

4.2 Monotonic Testing

All monotonic tests were run at a shearing normal stress of 692 kPa using the procedures described in Chapter 3. The displacement rates were 0.1, 1, 100, 10000, and approximately 25000 mm/min. The 0.1 mm/min test was an internal shear test, using an upper pullout plate with an aggressive metal teeth gripping system that forced internal failure of the GCL.

Figure 4.1 displays all of the shear stress-displacement plots for the monotonic tests. Many important trends can be gained from this plot. By far the largest peak strength is from the internal test that sheared was run at 0.1 mm/min. This test was completed to assess how close the GM/GCL interface was to possibly creating an interface failure. This test had an internal failure which resulted in the needle-punched fibers to be broken or pulled out. Failure of the reinforcement reduces the GCL shear strength to that of hydrated bentonite. This explains why the residual strength for this test was the lowest of all the tests. The GMX/GCL interface tests all follow the same general pattern. They quickly reach peak shear strength, τ_p, within a displacement of 20 mm. These specimens did not reach a residual within 220 mm of displacement, and this can be attributed to the fact that the specimens did not fail internally, but all exhibited interface failures. The large-displacement shear strength for these tests was obtained at a displacement of 200 mm, so for these tests $\tau_{ld} = \tau_{200}$. Overall, it is evident from this plot that the internal GCL failure had larger peak shear strengths and smaller residual shear strength than the GM/GCL interface failures.

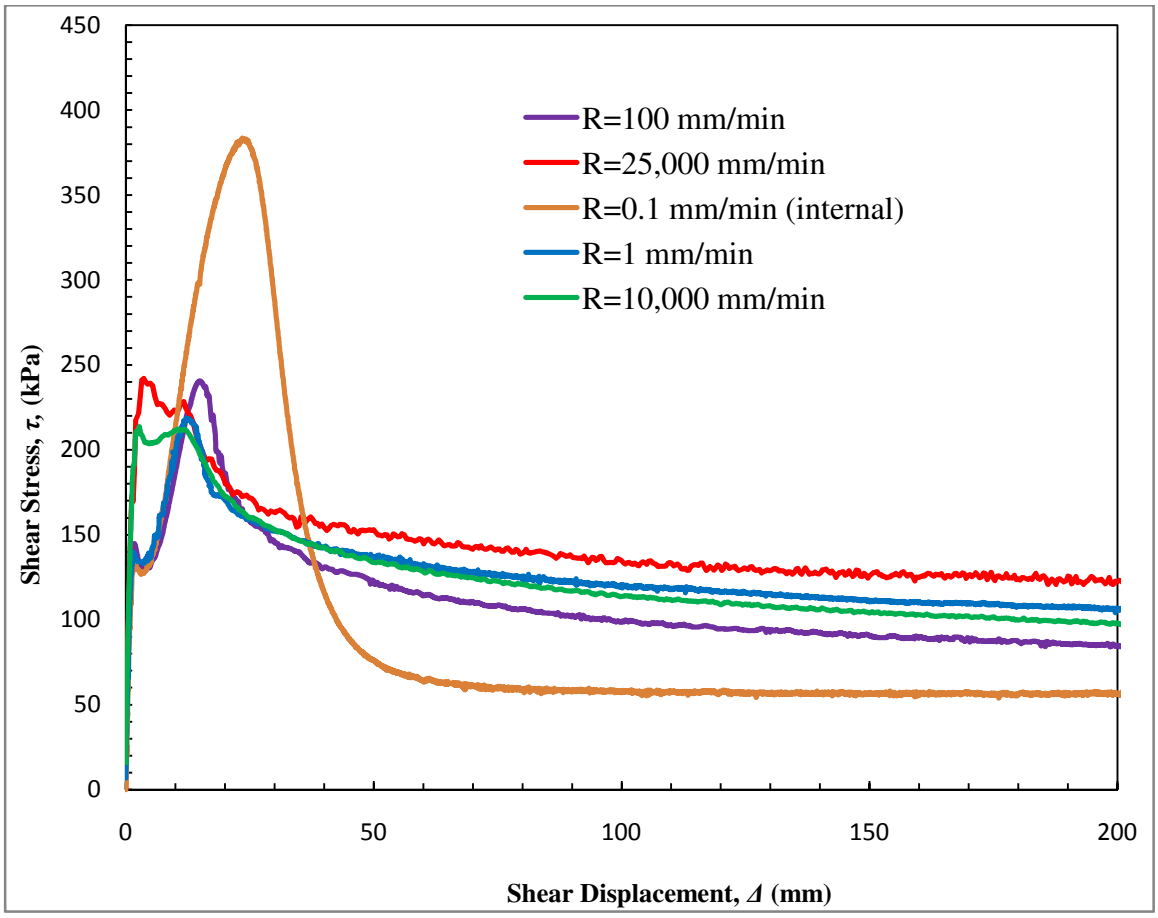

Figure 4.1: Shear stress vs. displacement for σ_n = 692 kPa.

Figure 4.2 displays a plot of τ_p and τ_{ld} versus displacement rate for R = 0.1 mm/min to R = 25,000 mm/min. It is important to remember that the 0.1 mm/min test was a GCL internal failure which results in the high peak and low residual strength. The smallest peak shear strength recorded was 212.2 kPa at R = 10,000 mm/min, and the largest shear strength was 241 kPa for R = 25,000 mm/min. This corresponds to only a 10% difference and suggests that displacement rate does not have a large effect on peak strength for the GMX/GCL interface. On the other hand, large-displacement shear strength decreases from R = 1 mm/min to R = 100 mm/min, and then increases to a

maximum value at R = 25,000 mm/min. The change from the highest to lowest value for the large-displacement strength is about 40%. This indicates that displacement rate may have an effect on the large-displacement shear strength of the GMX/GCL interface. The findings of this study are in general agreement with previous conclusions by Triplett and Fox (2001) that found there is no clear trend between displacement rate and shear strength for the GM/GCL interface. Figure 4.3 shows the displacement corresponding to peak strength for these tests. From this plot it can be observed that the displacement is far greater for the internal test than for the GCL/GMX interface. For the interface tests, there is not a clear trend in the relationship between displacement rate and displacement at peak, although with R = 25,000 mm/min the peak stress occurs at the smallest displacement.

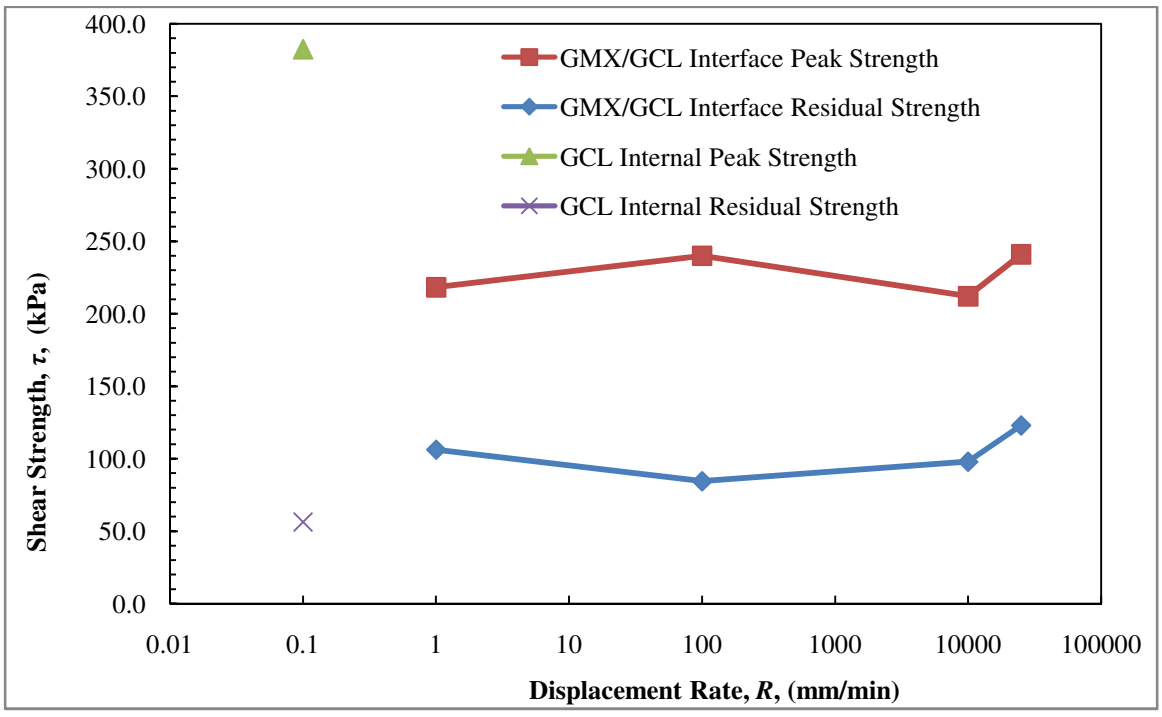

Figure 4.2: Peak strength and residual strength vs. displacement rate

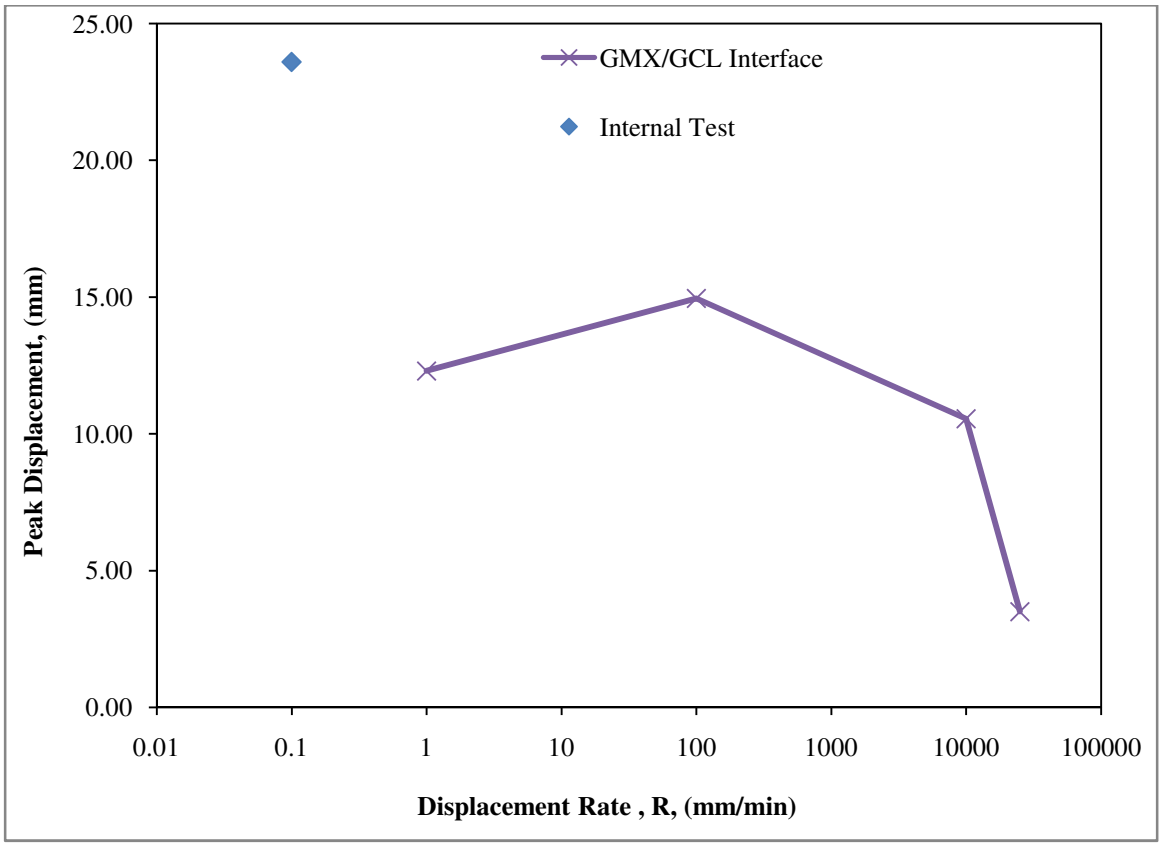

Figure 4.3: Effect of displacement rate on displacement at peak strength.

The plots of corresponding volume change for each monotonic test are shown in Figure 4.4. From this plot it can be observed that for all tests except R = 1 mm/min, the GCL specimen originally expanded, although this expansion was very small (<0.03 mm). All specimens underwent contraction at large displacements. The largest contract can be observed for R = 1 mm/min, with the other rates causing less contraction. The contraction for all interface tests is generally small (< 0.07 mm). It can also be observed that the internal test (R = 0.1 mm/min) had by far the greatest contraction.

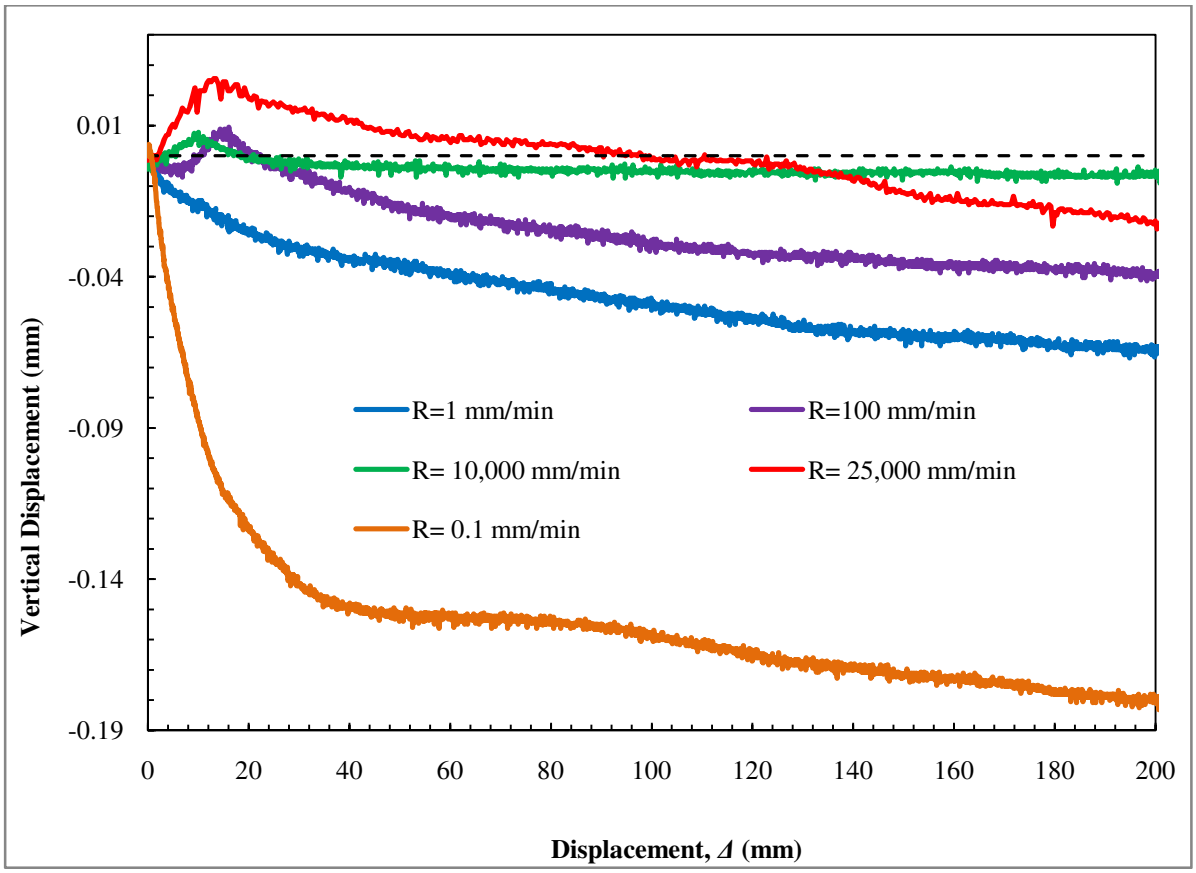

Figure 4.4: Volume change versus shear displacement for monotonic tests.

After the specimens underwent the monotonic testing procedure, they were removed from the testing chamber, and five water samples were cut from the centerline of each. The results of the water contents from each test are provided in Table 4.1. The average water content of the specimens was 73.4%, and the standard deviation and coefficient of variation were 9.9% and 13.4% respectively. The standard deviation gives a measure of the variability of the water content across the 5 samples, and the coefficient of variation is the ratio of the mean and standard deviation. For this data set, the low standard deviation and coefficient of variation imply that the water contents did not vary much across each specimen, which suggests the effective hydration.

Normal Stress (kPa)	Displacement Rate (mm/min)	Water content Measurements						Standard Deviation	Coefficient of Variation
		1	2	3	4	5	Mean		
692	0.1	84	75	65	65	66	71%	8.3%	11.7%
692	1	67	58	78	56	77	67%	10.2%	15.2%
692	100	57	76	85	96	77	78%	14.5%	18.6%
692	100	62	70	68	71	77	69%	5.3%	7.6%
692	10,000	76	67	74	73	85	75%	6.4%	8.6%
692	25,000	73	92	64	74	100	81%	14.8%	18.4%
		Average for all specimens:					73.4%	9.9%	13.4%

Table 4.1 Water content for each monotonic test.

4.3 Cyclic Testing

A cyclic testing program was completed on the GM/GCL interface at a normal stress of 692 kPa. The displacement amplitudes for the 7 tests were 2, 10, 15, 20, 30, 60, and 120 mm. The cyclic testing was performed using a sinusoidal wave form with a frequency of 1 Hz and carried out for 25 cycles. Figure 4.5 provides a plot of shear stress versus displacement for all seven tests. The first hysteresis loop starts at zero displacement and begins in the negative displacement direction, resulting in a negative shear force (tension). This explains why the largest shear strengths are observed to be in the third quadrant of the plot, because this is the first quarter-cycle of the cyclic test. The peak stress on the second-half of the first loop is smaller than the peak shear stress of the first quarter-cycle. This can be seen more clearly in Figure 4.6 which displays the shear

stress versus time for the displacement amplitude of Δ_a = 20 mm. In this figure it can be observed that the peak shear stress occurs during the first half of the first cycle, and then the peak shear stress decreases with each additional cycle. The greatest decrease in shear stress occurs between N = 1 and N = 10. After this point the stress reduction from each additional cycle is very small. This shows that after N = 10 cycles the strength reduction is negligible, and this agrees with Nye and Fox (2007) for a GCL internal failure.

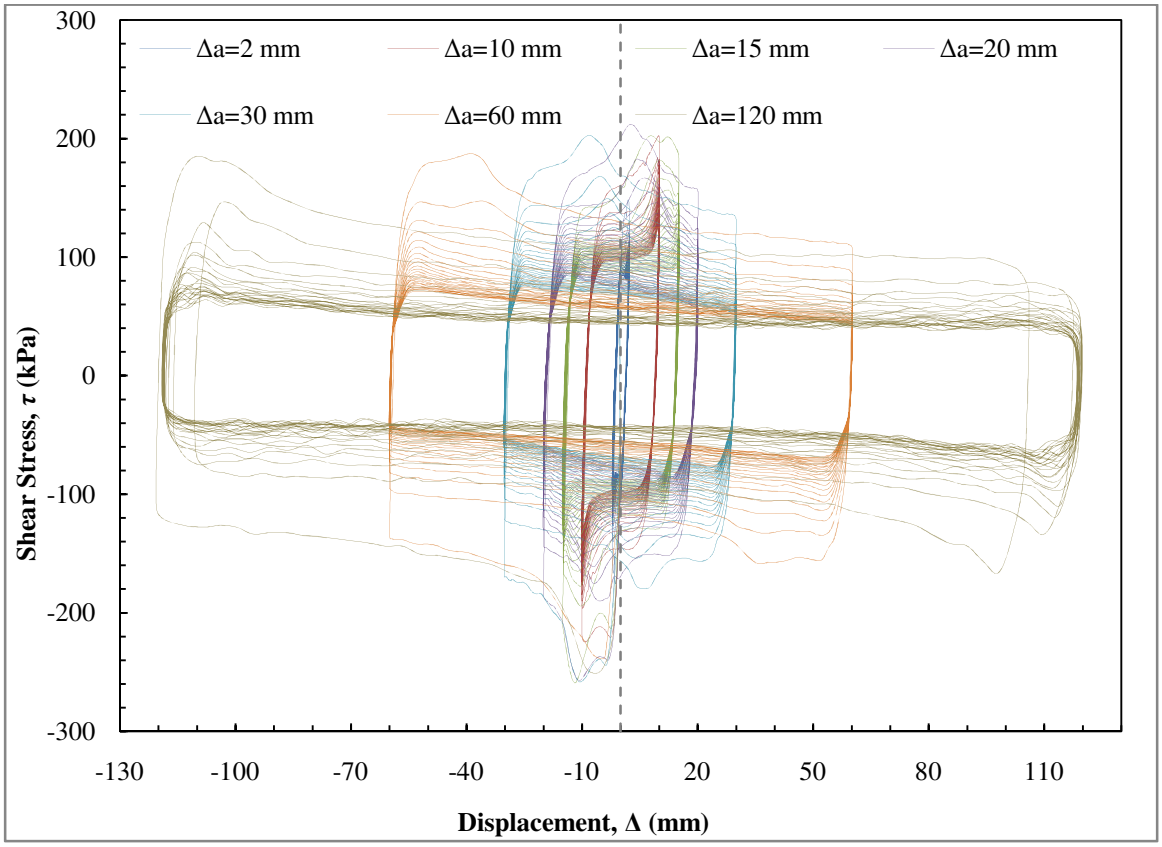

Figure 4.5: Shear stress versus displacement for seven cyclic shear tests.

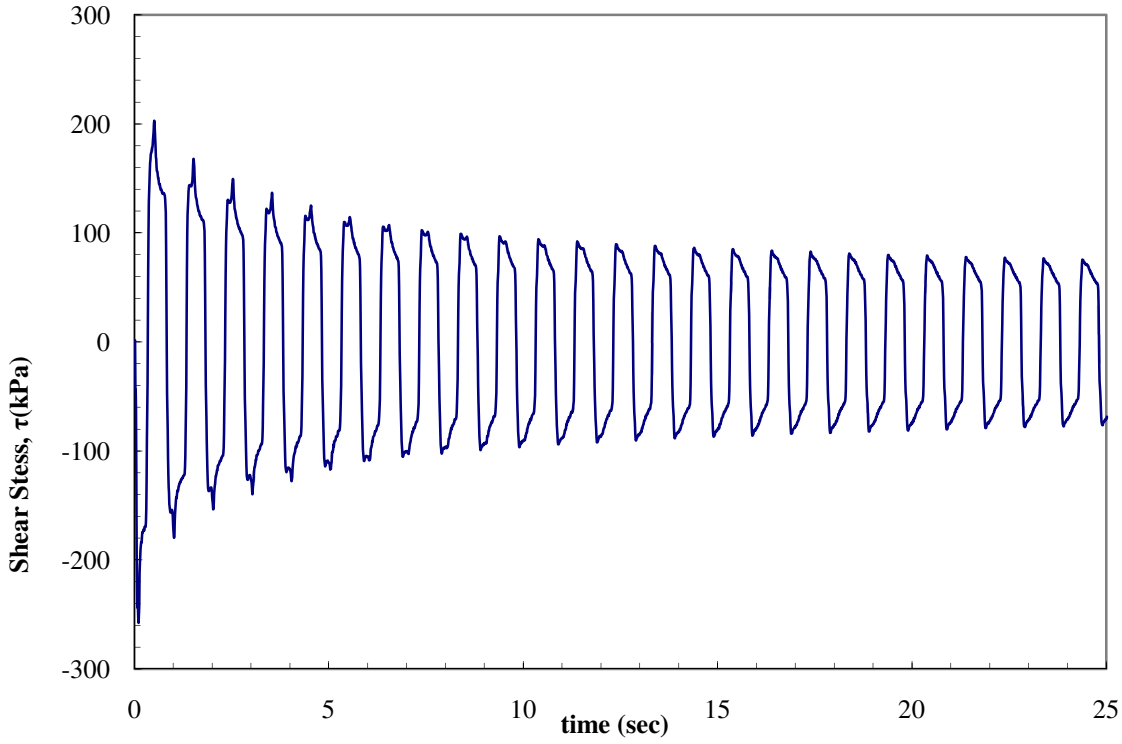

Figure 4.6: Shear stress for ± 30 mm cyclic shear test.

Figure 4.7 displays the first quarter-cycle of each hysteresis loop produced from the cyclic tests plotted against the R = 1 mm/min monotonic test. From this figure, it can be observed that the peak shear strength for the first quarter cycle of the cyclic test is generally larger than for the monotonic test. This can be attributed to the fact that the cyclic test moved at 1 Hz for each cycle which would result in a much faster rate than R = 1 mm/min. Referring back to Figure 4.3, it can be observed that the peak shear stresses are nearly equivalent or larger, and Figure 4.7 clearly displays this trend. It can also be observed from Figure 4.7 that although the peak shear strengths of the cyclic tests may be larger, they occur at approximately the same displacement. Also, the shear strengths for

the post-peak cyclic tests follow the shear strengths of the monotonic relatively closely at large displacements ($\Delta > 15$ mm).

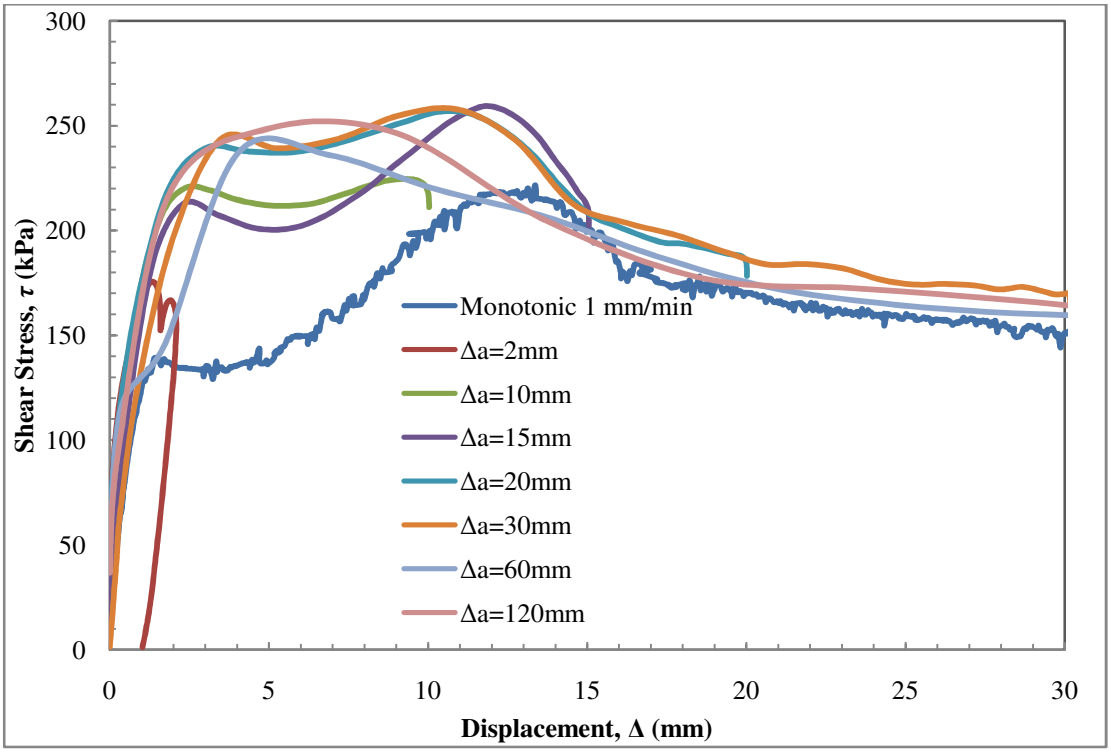

Figure 4.7: Shear stress versus displacement for first quarter cycle of seven cyclic tests.

Figure 4.8 shows the volume change behavior for each cyclic test. A positve vertical displacement resulted from the GMX/GCL specimen expansion, and a negative vertical displacement corresponds to specimen contraction. It can be observed that each specimen expanded during the first quarter cycle, but this expansion was less then 0.05 mm for each test. All specicimens experienced contraction between 0.1 and 0.15 mm by the end of the test. A portion of this contraction can be attributed to bentonite extruding

from the sides of the specimen during testing, but the majority is due to the cyclic loading. In general, greater displacment amplitudes caused greater specimen contraction during cyclic shear

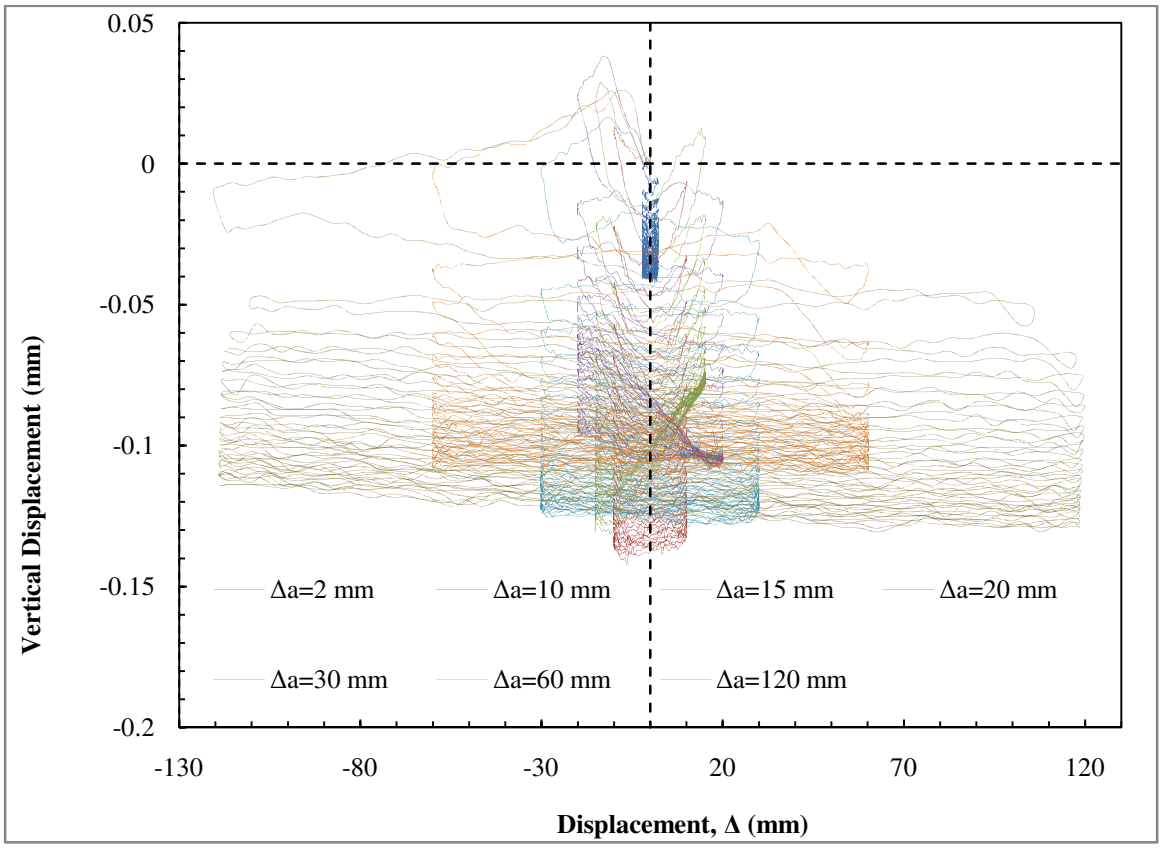

Figure 4.8: Volume change behavior during cyclic shear tests.

4.4 Post-Cyclic Shear Strength Testing

After the cyclic testing, the specimen was allowed a 24-hour rest period to contract or expand. All specimens displayed additional contraction during this rest period as indicated by the negative vertical displacement apperant in Figure 4.9. Each specimen then underwent static shearing at a constant displacement rate (R = 1 mm/min) which is the rate specified by ASTM D 6243 for direct shear tests of geosynthetic interfaces. Figure 4.10 displays the plot of shear stress versus displacement for all post-cyclic static shear tests, and the monotonic test with no previous cyclic testing (Δ_a = 0 mm). The Δ_a = 2 and 10 mm have very similar peak strength as the Δ_a = 0 mm. All tests with Δ_a greater then 10 mm have a peak strength that is reduced in comparison to the Δ_a = 0 mm test. This illustrates that a cyclic displacement of 10 mm or less does not have a significant effect on the peak shear strength of the GMX/GCL interface, but any cyclic displacement of 15 mm or more displays a large reduction in shear strength. For each cyclic test with displacement amplitudes of 15 mm or more, there is a decrease in peak shear strength with increasing displacement amplitude. However, at displacement amplitudes greater than Δ_a = 20 mm, futher increases in displacement amplitude caused only small reductions in post-cyclic peak shear strength. Altougth there is a reduction in the peak strength of tests that undergo large cyclic displacements, the peak strength for all tests occurs at similar displacements (10-20 mm). It should also be noted that with increasing cyclic displacement amplitude, the large-displacement shear strength during the monotonic test decreases. This results from the larger cyclic displacements causing more damage to the GMX/GCL interface.

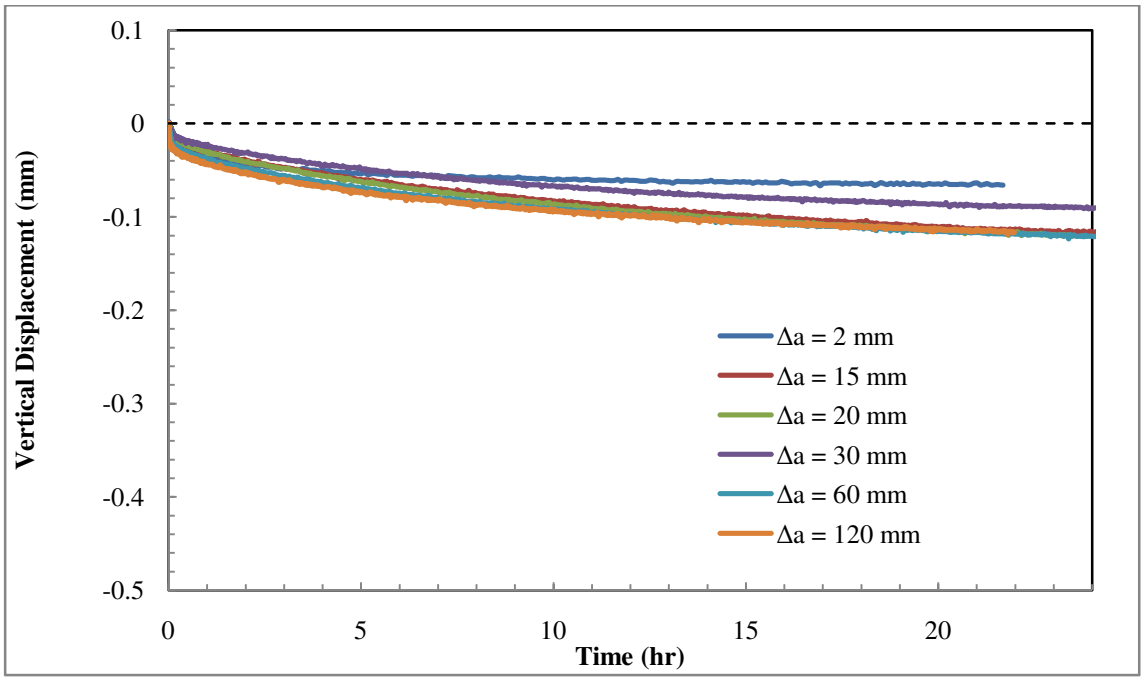

Figure 4.9: Second-stage hydration curves.

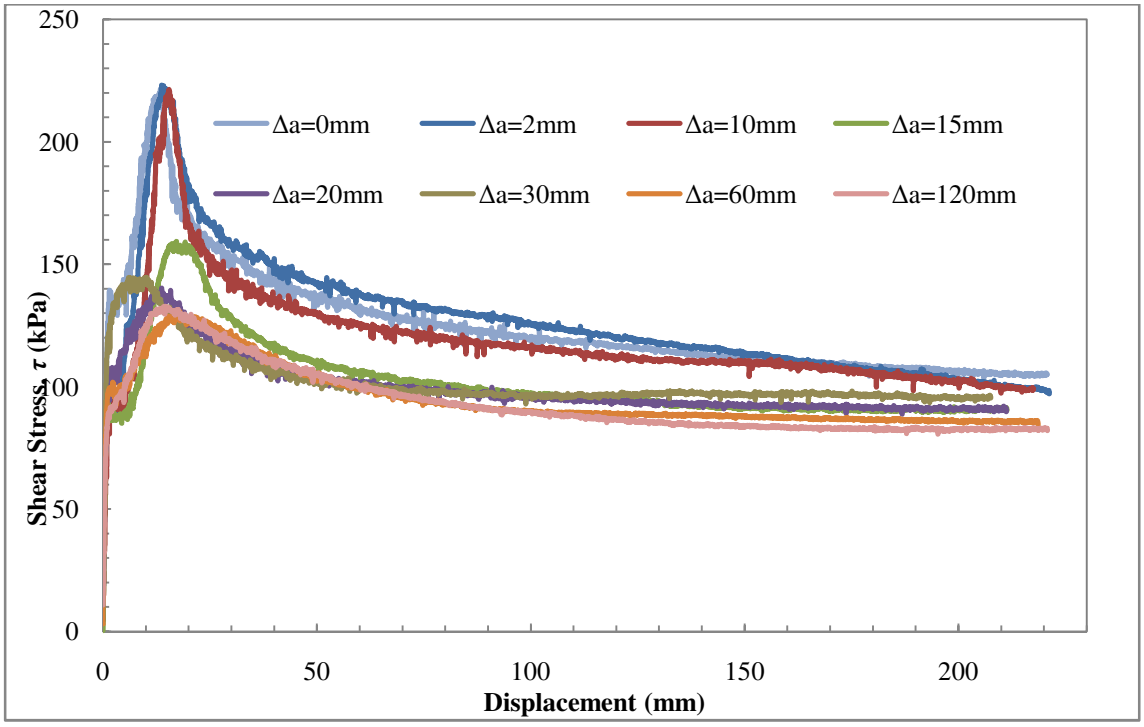

Figure 4.10: Effect of cyclic displacement amplitude on postcyclic monotonic shear behavior.

Figure 4.11 displays the volume change behavior during the post-cyclic static shear tests. In general, the specimens that underwent cyclic testing with amplitudes greater then 15 mm initially expanded before beginning contraction. All post-cyclic tests underwent contraction at large displacement. The tests with small cyclic displacement amplitudes underwent less specimen contraction during post-cyclic monotonic testing. This is because these specimens displayed larger contraction during cyclic testing than the smaller displacement amplitudes.

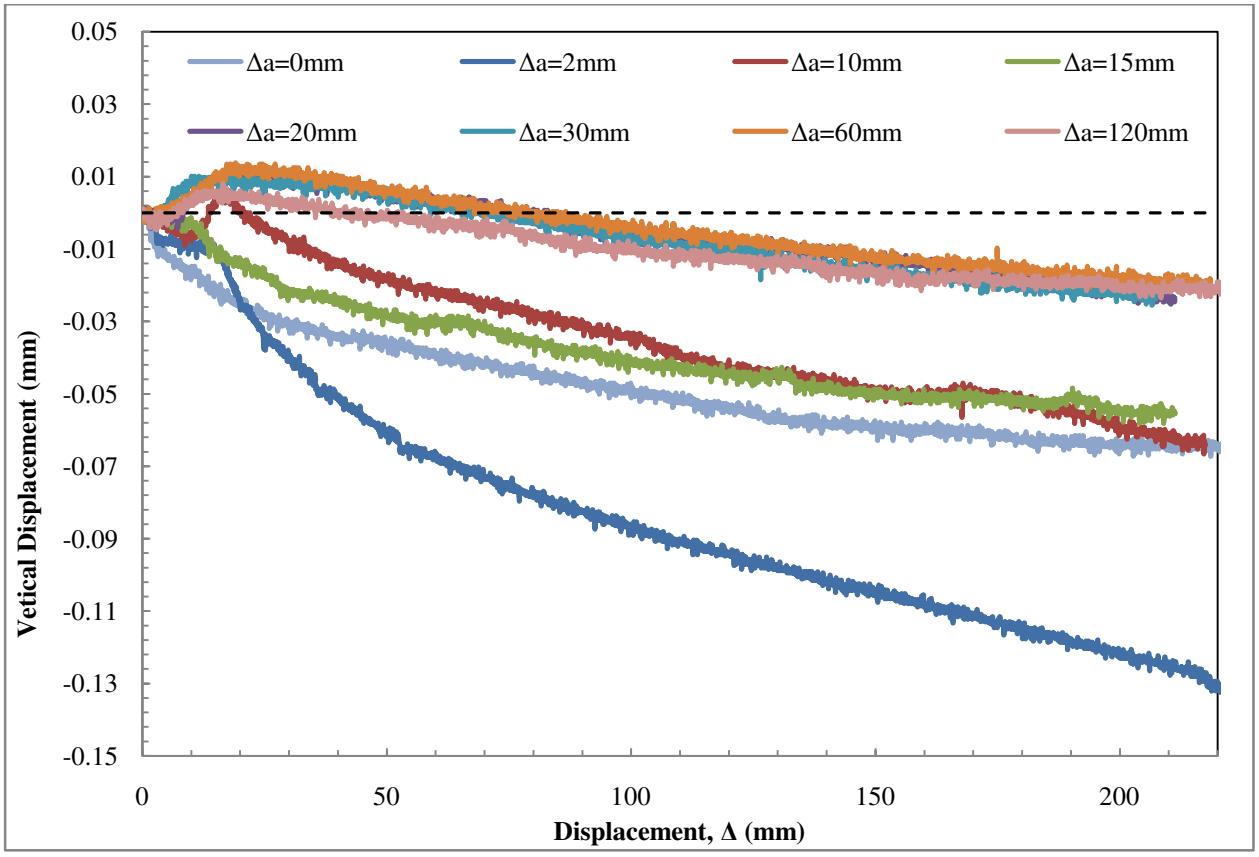

Figure 4.11: Volume change behavior for seven post-cyclic monotonic shear tests and one monotonic shear test without cyclic motion.

Table 4.1 presents the final water contents from the cyclic tests. The average water content was 59%, which is less then that found for the monotonic tests at the same normal stress. This is likely attributable to bentonite squeezing out the sides of the GCL during cyclic testing. Less bentonite in the GCL could possibly result in a smaller water content. The average standard deviation for the cyclic tests was 6.3%, indicating that there was relatively uniform distribution of water contents from the front to the back of the samples. The coefficient of varation was 10.8%, indicating that the water contents deviated ±10% from the average.

Normal Stress (kPa)	Cyclic Amplitude (mm)	Water Contents						Standard Deviation	Coefficient of Variation
		1	2	3	4	5	Mean		
692	2	60	57	56	67	65	61%	4.9%	8.0%
692	10	56	57	59	59	58	58%	1.3%	2.3%
692	15	61	58	65	66	52	60%	5.7%	9.4%
692	20	59	68	61	61	51	60%	6.0%	10.0%
692	30	54	58	52	53	83	60%	13.1%	21.7%
692	60	56	60	44	59	53	54%	6.2%	11.3%
692	120	59	55	56	70	50	58%	7.3%	12.6%
		Average for all specimens:					59%	6.3%	10.8%

Table 4.1: Water content measurements for cyclic shear specimens

CHAPTER 5

SUMMARY AND CONCLUSIONS

5.1 Introduction

The purpose of this research was to characterize the response of the GMX/GCL interface under monotonic and cyclic loading. In this chapter, each research area will be summarized, and the most important findings will be discussed in context with real world applications. Also, conclusions for the testing program will be made, and recommendations for future research will be discussed.

5.2 Monotonic Testing Conclusions

The following are the most important conclusions drawn from testing the GMX/GCL interface under monotonic shear loading:

1) Each specimen reached a peak shear strength within 20 mm of displacement, which was followed by a gradual post-peak strength reduction.

2) The displacement rate did not have a large effect on the peak shear strength.

3) The internal GCL shear strength test displayed larger peak shear strength and smaller large-displacement shear strength than the GMX/GCL interface tests.

4) In general, specimen contraction was observed for all montonic shear tests.

5) The average water content of the specimens after testing was 75.3% with a standard deviation of 9.9% and a coefficient of variation of 13.4%.

5.3 Cyclic Testing Conclusions

The following are the most important conclusions drawn from testing the GMX/GCL interface under cyclic loading:

1) The peak shear strength during each cyclic testing procedure occurred within the first quarter cycle, and showed continual reductions in shear strength for subsequent cycles.

2) A large amount of the shear strength reduction was observed in the first 10 cycles. After the 10^{th} cycle, only small reductions in shear strength were observed.

3) Comparing the first quarter-cycle of the hysteresis loop for the cyclic procedure to the R = 1 mm/min static test, it can be observed that the static test had a slightly lower peak strength. This can likely be attributed to the larger displacement rates of the cyclic tests.The peak strength occurred at approximitely the same displacement for all cyclic tests. Also, post-peak shear strengths of the monotonic and cyclic tests were very comparable.

4) All specimens originally expanded (>0.05 mm) before undergoing contraction. The larger the displacement amplitude, the larger the original expanded and eventual contraction of the specimen during cyclic shear.

5.4 Post-Cyclic Shear Strength Conclusions

The following are the most important conclusions drawn from testing the GMX/GCL interface under post-cyclic static shear testing:

1) The Δ_a = 2 and Δ_a = 10 mm displacement amplitude specimens displayed same peak strength as the Δ_a = 0 mm (no cyclic) static test. The post-cyclic tests (Δ_a = 2 and 10 mm) displayed smaller large-displacement shear strengths than the static test.

2) For tests with $\Delta_a > 10$ mm, the peak shear strength is greatly reduced compared to the $\Delta_a = 0$ mm static test.

3) As the displacement amplitude increases, the static peak strength decreases, but all tests display similar large-displacement shear strengths.

4) For $\Delta_a > 15$ mm the specimen orginally expanding, but after large displacements, all specimens underwent contraction.

5) The post-cyclic test specimens displayed less contraction during the post-cyclic static test than the specimen that did not undergo cyclic motion. This is attributable to the contraction that had already occurred during cyclic motion for the post-cyclic test specimens.

6) The water content, standard deviation, and coeffiecient of variation for were 59%, 6.3%, and 10.8%, respectively.

7) It may be ascertained from the cyclic results that earthquake displacements along the interface that are less than 10 mm, may not cause shear strength reductions. However, large dispalcements ($\Delta_a > 10$ mm) will cause large reductions in shear strength on the GM/GCL interface.

5.5 Recommendations for Future Research

The research that was discussed in this thesis is extremely important to characterize the response of GMX/GCL interface under dynamic loading. However, this

research only considered a small portion of materials available for use in landfill liner systems, and a very specific normal stress and testing conditions. The following are suggestions for future research that would provide a strong contribution to the topic of shear strength of geosynthetics.

1) The same testing program needs to be completed on different landfill interfaces, including different types of GMs and GCLs. Specifically, the response of a GMX with a compacted clay liner should be considered.

2) The landfill liner system is designed to last for hundreds of years, but the amount of information avaiblable to describe the long-term effects, (i.e. creep or GCL durability), is not well known. Therefore, there is a need for long-term strength testing of geosynthetics.

3) A wider range of displacement rates should be utilitized in the monotonic direct shear tests. This would allow a better quantificaiton of the effect of peak and large-displacement shear strength within a constant normal stress. This should include rates slower than 1 mm/min.

REFERENCES

Fox, P.J., Nye, C.J., Morrison, T.C., Hunter, J.G., and Olsta, J.T. (2006). "Large dynamic direct shear machine for geosynthetic clay liners." *Geotechnical Testing Journal,* 29(5). 1-9.

Fox, P.J., Rowland, M.G., and Scheithe, J.R., (1998). "Internal shear strength of three geosynthetic clay liners." *Journal of Geotechnical and Geoenvironmental Engineering,* 124(10), 933-944.

Fox, P.J., Rowland, M.G., Scheithe, J.R., Davis K.L., Supple M.R., and Crow, C.C., (1997). "Design and evaluation of a large direct shear machine for geosynthetic clay liners." *Geotechnical Testing Journal.* 20(3), 279-288.

Fox, P. J., and Stark, T.D. (2004) "State-of-the-art report: GCL shear strength and its measurements." *Geosynthetics International,* 11(3), 141-174.

Gilbert, R.B., Fernandez, F. and Horsfield, D.W. (1996). "Shear Strength of reinforced geosynthetic clay liner." *Journal of Geotechnical Engineering,* 122(4), 259-266.

Kim, J., Riemer, M., and Bray, J.D. (2005). "Dynamic properties of of geosynthetic interfaces." *Geotechnical Testing Journal,* 28(3), 1-9.

Lai, J., Daniel, D. E. and Wright, S. G. (1998). "Effects of cyclic loading on internal shear strength of unreinforced geosynthetic clay liner." *Journal of Geotechnical and Geoenvironmental Engineering,* 124(1), 45-52.

Lo Grasso, S.A., Massimino, M.R., and Maugeri, M. (2002). "Dynamic analysis of geosynthetic interfaces by shaking table tests." Proc., 7th International Conference on Geosynthetics, P. Delmas and J.P. Gourc, eds., 4, Nice, 1335-1338.

Nye, C. J. (2007). Research on the dynamic internal shear behavior of a needle-punched geosynthetic clay liner. Unpublished Master's Thesis. The Ohio State University, Columbus.

Nye, C.J., and Fox, P.J. (2007). "Dynamic shear behavior of a needle-punched geosynthetic clay liner." *Journal of Geotechnical and Geoenvironmental Engineering*. 133(8), 973-983.

Stark, T.D., and Eid, P.J. (1996). "Shear behavior of reinforced geosynthetic clay liners." *Geosynthetics International*, 3(6), 771-786.

Sura, J. M. (2009). Monotonic and cyclic shear response of a needlepunched geosynthetic clay liner and high normal stresses. Unpublished Master's Thesis. The Ohio State University, Columbus.

Triplett, E. J., and Fox, P. J. (2001). "Shear strength of HDPE geomembrane/geosynthetic clay liner interfaces." *Journal of Geotechnical and Geoenvironmental Engrineering,* 127(6), 543-552.

APPENDIX A

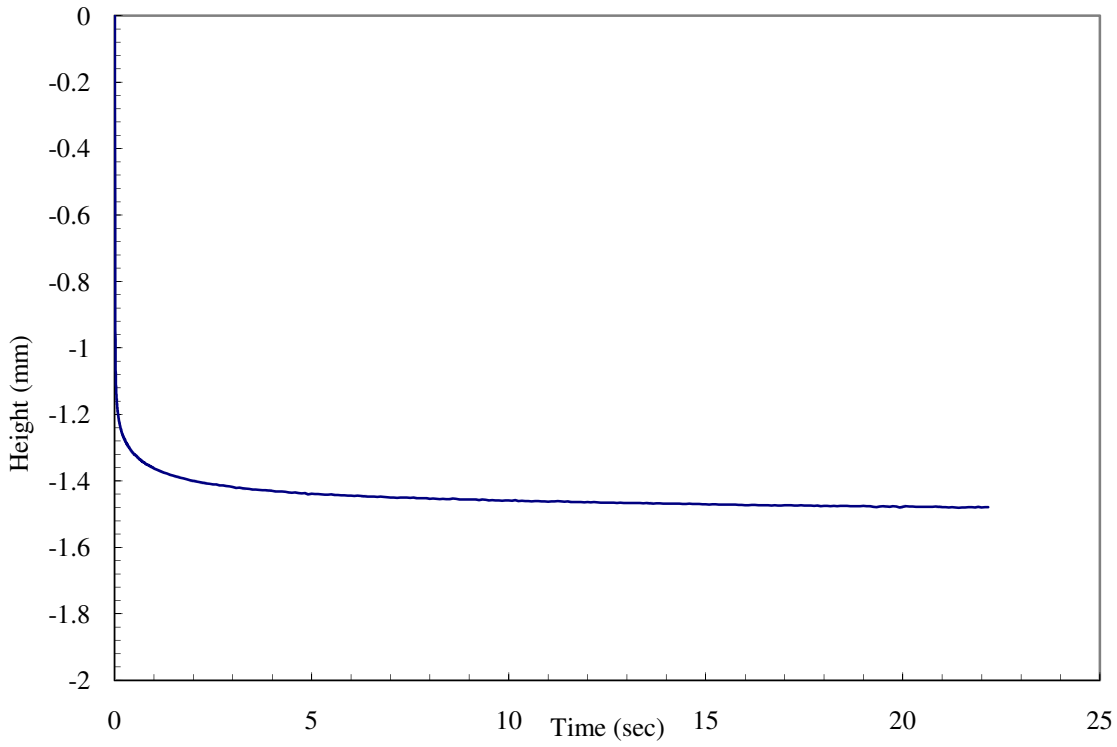

Figure A.1: Typical hydration curve for 2nd stage of hydration procedure.